Chapter U

Reflection-mode ultrasound imaging

Contents

Introduction to real-time reflection-mode ultrasound imaging

Outline

- Overview
- Source: Pulse and attenuation
- Object: Reflectivity
- Geometric imaging (PSF approximation)
- Diffraction: Fresnel and Fraunhofer approximations
- Noise
- Phased-arrays (beamforming, dynamic focusing)
- R, θ scan conversion

Overview

- Ultrasound: acoustic waves with frequency > 20kHz. Medical ultrasound typically 1-10MHz.
- Ultrasound imaging is fundamentally a non-reconstructive, or direct, form of imaging. (Minimal post-processing required.)
- Two-dimensions of spatial localization are performed by diffraction, as in optics.
- One-dimension of spatial localization is performed by pulsing, as in RADAR.
- The ultrasonic wave is created and launched into the body by electrical excitation of a piezoelectric transducer.
- Reflected ultrasonic waves are detected by the same transducer and converted into an electrical signal.
- Basic ultrasound imaging system is shown below.

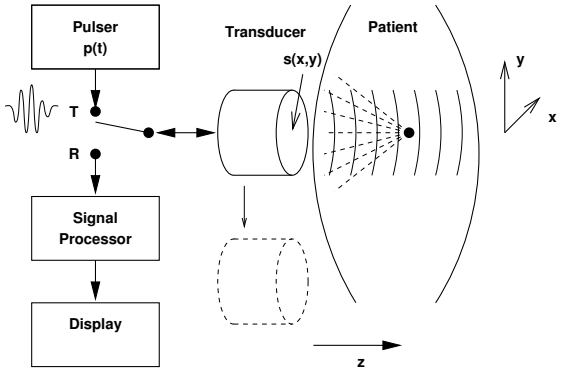

- A pulser excites the transducer with a short pulse, often modeled as an amplitude modulated sinusoid: $p(t) = a(t)\,\mathrm{e}^{-\imath\omega_0 t}$, where $\omega_0 = 2\pi f_0$ is the **carrier frequency**, typically 1-10 MHz.
- The ultrasonic pulse propagates into the body where it reflects off *mechanical inhomogeneities*.
- Reflected pulses propagate back to the transducer. Because distance = velocity $\times$ time, a reflector at distance z from the transducer causes a pulse "echo" at time $t = \frac{2z}{c}$, where c is the sound velocity in the body.
- Velocity of sound about 1500 m/s $\pm 5\%$ in soft tissues of body; very different in air and bone.
- Reflected waves received at time t are associated with mechanical inhomogeneities at depth $z = ct/2$.
- The **wavelength** $\lambda = c/f_0$ varies from 1.5 mm at 1 MHz to 0.15 mm at 10 MHz, enabling good depth resolution.
- The cross-section of the ultrasound "beam" from the transducer at any depth z determines the lateral extent of the echo signal. The beam properties vary with range and are determined by diffraction. (Determines PSF.)
- We obtain one line of an image simply by recording the reflected signal as a function of time.
- 2D and 3D images are generated by moving the direction of the ultrasound beam.
- Signal processing: bandpass filtering, gain control, envelope detection.

History

- started in mid 1950's
- rapid expansion in early 1970's with advent of 2D real-time systems
- phased arrays in early 1980's
- color flow systems in mid 1980's
- 3D systems in 1990's
- Active research field today including contrast agents (bubbles), molecular imaging, tissue characterization, nonlinear interactions, integration with other modalities (photo-acoustic imaging, combined ultrasound / X-ray tomosynthesis)

Example.

A month later...

Object: What does ultrasound image?

Reflection-mode ultrasound images display the **reflectivity** of the object, denoted $R(x, y, z)$.
The reflectivity depends on both the object shape and the material in a complex way.
Two important types of reflections are **surface reflections** and **volumetric scattering**.

Surface reflections or specular reflections

Large planar surface (relative to wavelength λ), *i.e.*, planar boundary between two materials of different acoustic impedances.
(*e.g.*, waves in swimming pool reflecting off of concrete wall)

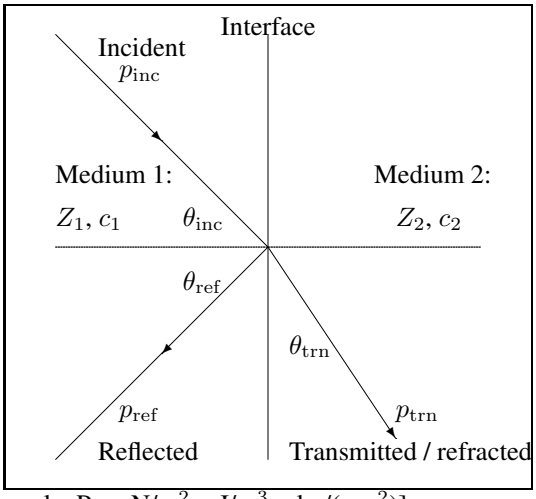

- p is **pressure** (force per unit area) [Pascals: Pa = N/m^2 = J/m^3 = kg/(m s^2)]
- v is **particle velocity** [m/s]. p and v are signed scalar quantities that can vary over space and with time.
- $Z = p/v$ is **specific acoustic impedance** [kg/(m^{2}s)] (analogous to Ohm's law: resistance = voltage / current)
- For a plane harmonic wave: $Z = \rho_0 c$, called **characteristic impedance**
- ρ_0 is **density** [g/m^3]
- c is (wave) **velocity** [m/s]
- Force: 1 dyne = 1 g cm / s^2, 1 newton = 1 kg m / s^2 = 1·10^6 dyne

Boundary conditions [2, p. 88]:
- Equilibrium total pressure at boundary: $p_{\text{ref}} + p_{\text{inc}} = p_{\text{trn}}$
  Total pressure left of interface is $p_{\text{ref}} + p_{\text{inc}}$, and "pressure must be continuous across interface" [3, p. 324].
- Snell's law: $\sin\theta_{\text{inc}} / \sin\theta_{\text{trn}} = c_1/c_2$
- Continuous particle velocity: $v_{\text{inc}} \cos\theta_{\text{inc}} = v_{\text{ref}} \cos\theta_{\text{ref}} + v_{\text{trn}} \cos\theta_{\text{trn}}$
- Angle of reflection: $\theta_{\text{ref}} = -\theta_{\text{inc}}$ (like a mirror).

From the picture we see that $Z_1 = p_{\text{inc}} / v_{\text{inc}}$, $Z_1 = p_{\text{ref}} / v_{\text{ref}}$, $Z_2 = p_{\text{trn}} / v_{\text{trn}}$. Substituting into particle velocity condition:

$$\left(\frac{p_{\text{inc}}}{Z_1} - \frac{p_{\text{ref}}}{Z_1} \right) \cos\theta_{\text{inc}} = \frac{p_{\text{trn}}}{Z_2} \cos\theta_{\text{trn}} \quad \text{so } 1 + R = \frac{\cos\theta_{\text{inc}}}{\cos\theta_{\text{trn}}} \frac{Z_2}{Z_1} (1 - R).$$

Thus the **pressure reflectivity** at the interface is

$$\boxed{R = \frac{p_{\text{ref}}}{p_{\text{inc}}} = \frac{Z_2 \cos\theta_{\text{inc}} - Z_1 \cos\theta_{\text{trn}}}{Z_2 \cos\theta_{\text{inc}} + Z_1 \cos\theta_{\text{trn}}}.}$$

Only surfaces parallel to detector (or wavefront) matter (others reflect away from transducer), so $\theta_{\text{inc}} = \theta_{\text{ref}} = \theta_{\text{trn}} = 0$. Thus the **reflectivity** or **pressure reflection coefficient** for waves at normal incidence to surface is:

$$\boxed{R = R_{12} = \frac{p_{\text{ref}}}{p_{\text{inc}}} = \frac{Z_2 - Z_1}{Z_1 + Z_2} \approx \frac{\Delta Z}{2 Z_0},}$$

where Z_0 denotes the typical acoustic impedance of soft tissue. Clearly $-1 \le R \le 1$, and R is unitless. Note that $R_{21} = -R_{12}$.

Typically $\frac{\Delta Z}{Z_0}$ is only a few % in soft tissue, so **weakly reflecting** (not much energy loss). But "shadows" occur behind bones.

Also useful is the **pressure transmittivity** or **pressure transmission coefficient**:

$$\tau_{12} = \frac{p_{\text{trn}}}{p_{\text{inc}}} = \frac{p_{\text{inc}} + p_{\text{ref}}}{p_{\text{inc}}} = 1 + R_{12} = \frac{2Z_2}{Z_1 + Z_2} \approx 1.$$

Note that $\tau_{21} = 1 + R_{21} = 1 - R_{12}$.

It is fortunate that $\tau_{12} \approx 1$! Ultrasound would be much more difficult otherwise.

Surface reflections are an **extrinsic** property, because they are related to the *relative* impedances between two tissues, rather than representing just the characteristics of a single tissue.

The **intensity** of an ultrasonic wave is $I = p^2/(2Z)$. Thus the reflected and transmitted intensities are

$$I_{\text{ref}}/I_{\text{inc}} = \left(\frac{Z_2 - Z_1}{Z_2 + Z_1}\right)^2, \quad I_{\text{trn}}/I_{\text{inc}} = \frac{4Z_2Z_1}{(Z_2 + Z_1)^2}.$$

Note that $I_{\text{inc}} + I_{\text{ref}} = I_{\text{trn}}$ as one would expect.

Volumetric Scattering

On a microscopic level (less than or comparable to an ultrasonic wavelength), mechanical inhomogeneities inherent in tissue will scatter sound.

Individual inhomogeneities are less than an ultrasound wavelength and distributed throughout the volume.

$\eta =$ Backscatter coefficient = Backscatter cross section/unit volume

These volumetric signals are very weak (typically 20 dB down from surface reflections) but are very useful for imaging because they are an **intrinsic** property of the microstructure of tissue.

Volumetric scattering is **nearly isotropic** so that the backscattered component is always present and is representative of the tissue.

Volumetric scattering can give rise to **speckle**.

Can we see a tumor using ultrasound? **??**

Summary

In reflection-mode ultrasound imaging, the images are "representative reproductions" of the **reflectivity** of the object. A cyst, which is a nearly homogeneous fluid-filled region, has reflectivity nearly 0, so appears black on ultrasound image. Liver tissue, which has complicated cellular structure with many small mechanical inhomogeneities that scatter the sound waves, appears as a fuzzy gray blob (my opinion). Boundaries between organs or tissues with different impedances appear as brighter white curves in the image.

Preview of A-mode scan

- Assume the medium has a *uniform sound speed* c and is **weakly reflecting**, so we ignore 2nd order and higher reflections.
- Also ignore (for now) attenuation.
- Assume the transducer transmits an amplitude modulated pulse $p(t) = a(t)\,\mathrm{e}^{\imath\omega_0 t}$, where $\omega_0 = 2\pi f_0$ is the **carrier frequency** and $a(t)$ is the **envelope**. In reality the modulation is sinusoidal, and one uses I,Q receiver processing for envelope detection.

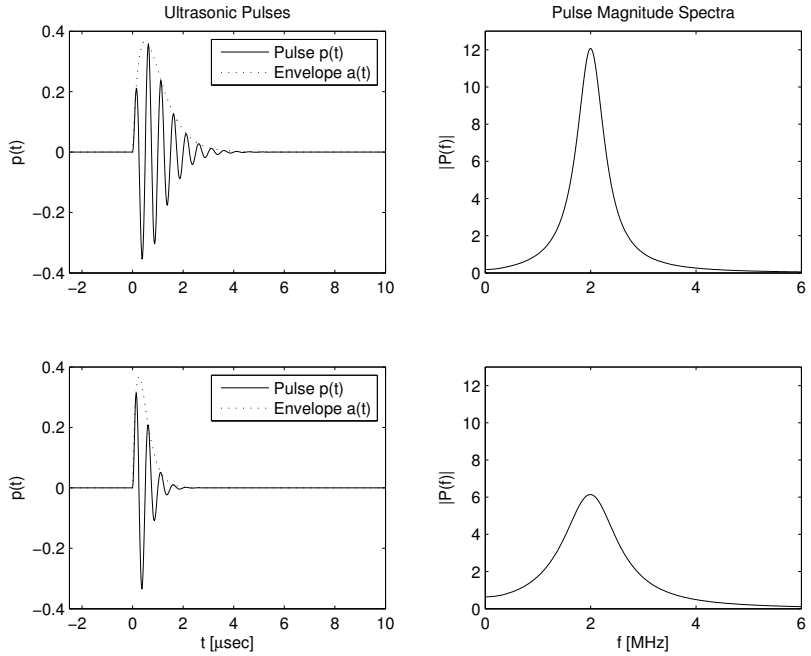

- Suppose at depths $z_1, \ldots, z_N$ there are interfaces with reflectivities $R(z_1), \ldots, R(z_N)$, *i.e.*,

$$R(z) = \sum_{n=1}^{N} R(z_n)\,\delta(z - z_n)\,. \textbf{ (Picture)}$$

- Then a (highly simplified) model for the signal received by the transducer is:

$$v(t) = K \sum_{n=1}^{N} R(z_n)\,p(t - 2z_n/c), \textbf{ (Picture)}$$

  where K is a constant gain factor relating to the impedance of the transducer, electronic preamplification, etc.
- A natural estimate of the reflectivity is

$$\hat{R}(z) = \left| v\left(\frac{2z}{c}\right) \right|, \textbf{ (Picture)}$$

  where $|v(t)|$ is the **envelope** of the received signal.

One can display the estimated reflectivity $\hat{R}(z)$ as a function of depth z, simply by "synchronizing the display device" to show the amplitude of the received envelope signal $|v(t)|$ (*e.g.*, analog scope trace). It is a plot of *amplitude* versus time (or depth), hence it is called an **A-mode scan**. Can be completely analog (and it was in early days).

Is $\hat{R}(z) = R(z)$? No. Even in this highly simplified model, there is blurring (in z direction) due to the width of the pulse. Soon we will analyze the blur in all directions more thoroughly.

Also note that reflection coefficients can be positive or negative, but with envelope detection we lose the sign information. Hereafter we will ignore this detail and treat reflectivity R as a nonnegative quantity.

What happens if sound velocity in some organ differs from others?

Synopsis of M-mode scan

If reflectivity is a function of time t, *e.g.*, due to cardiac motion, then we have $R(z;t)$. If the time scale is slow compared to A-mode scan time (300 μsec), then just do multiple A-mode scans (1D) and stack them up to make 2D "image" of $\hat{R}(z,t)$.

Illustration of A-mode scan

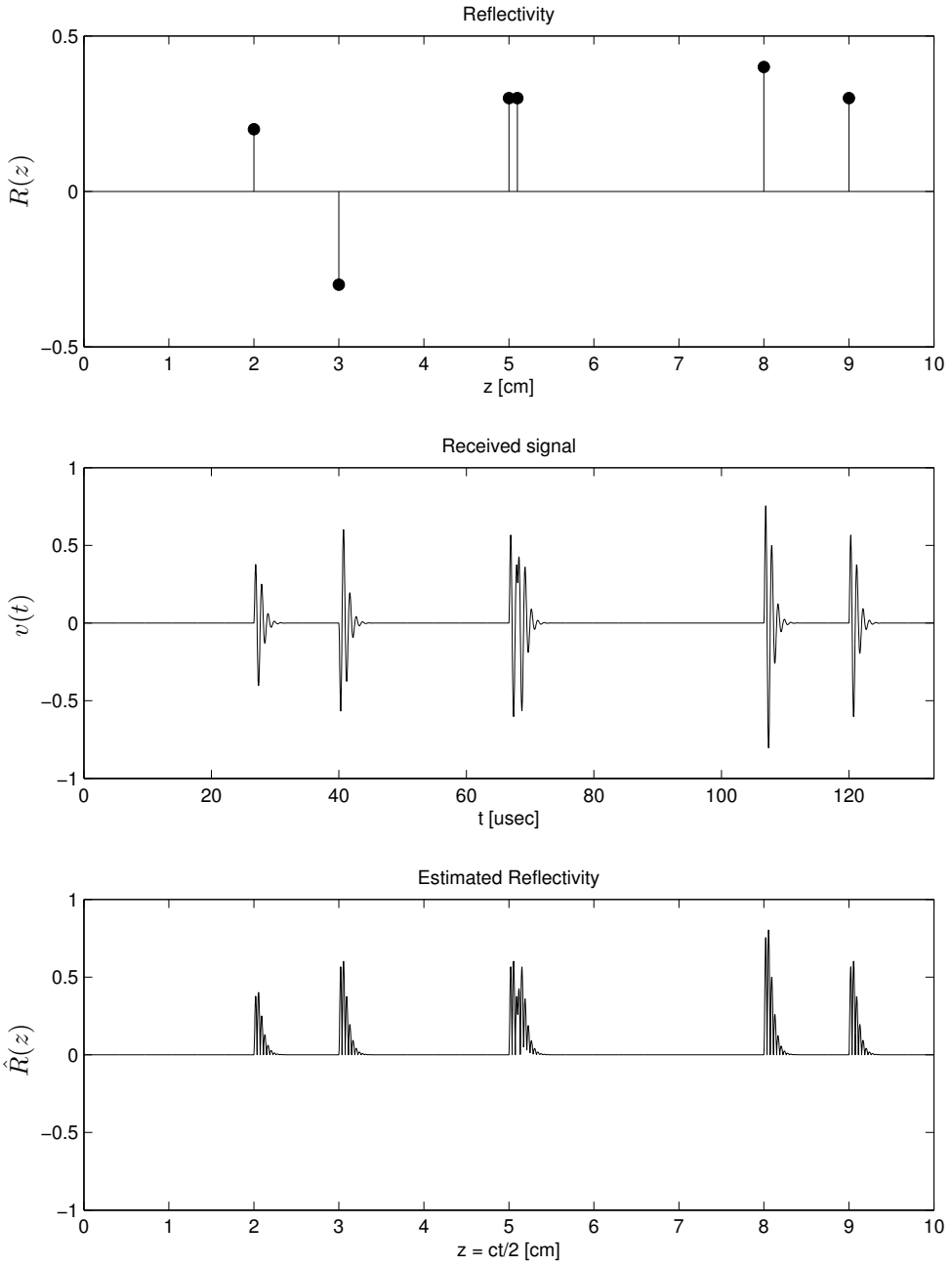

- $z = ct/2$ (distance = rate $\times$ time, depth = distance / 2)
- depth resolution vs pulse width
- speckle
- scan speed

Plane wave propagation

Assume a medium that is homogeneous, continuous, of infinite extent, and nondissipative (*i.e.*, no energy is lost as the sound wave propagates).

In ideal fluids (and for practical purposes in soft tissue), only **longitudinal waves** are propagated, *i.e.*, the particles of the medium are displaced from their equilibrium position in the direction of wave propagation only. **Transverse waves**, or **shear waves** cannot be generated in an ideal fluid (essentially by definition of an ideal fluid).

If $p(x,y,z,t)$ denotes the (acoustic) pressure at spatial coordinates (x,y,z) at time t, then after various linearizations (*i.e.*, for small pressure changes) one can derive the **simple wave equation** which must hold away from sources:

$$\boxed{\nabla^2 p - \frac{1}{c^2}\frac{\partial^2}{\partial t^2} p = 0}$$

where

$$\nabla^2 = \frac{\partial^2}{\partial x^2} + \frac{\partial^2}{\partial y^2} + \frac{\partial^2}{\partial z^2}.$$

Replacing ∇^2 with $\frac{\partial^2}{\partial z^2}$ yields the 1D wave equation, which has general solution

$$p(z,t) = \phi_{\text{forward}}(t - z/c) + \phi_{\text{backward}}(t + z/c),$$

where ϕ_{forward} and ϕ_{backward} are arbitrary twice differentiable functions.
Note that z/c is the time required to for the wave to propagate the distance z.

One specific class of solutions to this equation is the "monochromatic" plane wave with frequency f:

$$p_f(z,t) = P(f)\, \mathrm{e}^{\imath 2\pi f(t - z/c)}$$

where $P(f)$ is the amplitude, for which $\phi_{\text{backward}} = 0$. It is a simple calculus exercise to verify that

$$\nabla^2 p = \frac{1}{c^2}\frac{\partial^2}{\partial t^2} p = -\frac{(2\pi f)^2}{c^2} p = -k^2 p$$

where $\boxed{k = 2\pi f/c = 2\pi/\lambda}$ is called the **wave number**. This confirms that plane waves satisfy the wave equation.

Because the simple wave equation is linear, any superposition of solutions is also a solution. Hence

$$p(z,t) = \int p_f(z,t)\, \mathrm{d}f = \int P(f)\, \mathrm{e}^{\imath 2\pi f(t - z/c)}\, \mathrm{d}f$$

is also a solution. Observe that $p(z,t) = p(0, t - z/c)$ where $p(0,t) = \int P(f)\, \mathrm{e}^{\imath 2\pi f t}\, \mathrm{d}f = \mathcal{F}^{-1}\{P\} = p(t)$.

Spherical waves

Another family of solutions to the wave equation is

$$p(r,t) = \frac{1}{r}\phi_{\text{outward}}(t - r/c) + \frac{1}{r}\phi_{\text{inward}}(t + r/c),$$

where $r = \sqrt{x^2 + y^2 + z^2}$.

A specific case is the spherical wave:

$$p(r,t) = \frac{1}{r}\, \mathrm{e}^{\imath 2\pi f(t - r/c)}\,.$$

Using the equality $\frac{\partial}{\partial x} r = x/r$, one can verify that:

$$\nabla^2 p = \frac{1}{c^2}\frac{\partial^2}{\partial t^2} p = -k^2 p(r,t).$$

Source considerations

Now we begin to examine the considerations in designing the transducer and the transmitted pulse.

Transducer considerations

- Definition of **transducer**: a substance or device, such as a piezoelectric crystal, microphone, or photoelectric cell, that converts input energy of one form into output energy of another.
- Transducer electrical impedance $\propto$ 1/area, so smaller source means more noise (but better near-field lateral spatial resolution).
- Higher carrier frequency means wider filter after preamplifier, so more noise (but better depth resolution).
- Nonuniform gains for each element must be calibrated; errors in gains broaden PSF.

Pulse considerations (Why a pulse? And what type?)

Consider an ideal infinite plane-reflector at a distance z from the transducer, and an acoustic wave velocity c.
If the transducer transmits a pulse $p(t)$ (pressure wave), then (ignoring diffraction) ideally the received signal (voltage) would be

$$v(t) = p\left(t - \frac{2z}{c}\right),$$

because $\frac{2z}{c}$ is the time required for the pulse to propagate from the transducer to the reflector and back.

Unfortunately, in reality the amplitude of the pressure wave decreases during propagation, and this loss is called **attenuation**. It is caused by several mechanisms including **absorption** (wave energy converted to thermal energy), **scattering** (generation of secondary spherical waves) and **mode conversion** (generation of transverse shear waves from longitudinal waves).

As a further complication, the effect of attenuation is *frequency dependent*: higher frequency components of the wave are attenuated more. Thus, it is natural to *model* attenuation in the frequency domain to *analyze* what happens in the time domain.

Ideally the recorded echo could be expressed using the 1D inverse FT as follows

$$v(t) = p\left(t - \frac{2z}{c}\right) = \int P(f)\, \mathrm{e}^{\imath 2\pi f (t - \frac{2z}{c})}\, \mathrm{d}f\,.$$

A more realistic (phenomenological) *model* (but still ignoring frequency-dependent wave-speed) accounts for the frequency-dependent attenuation as follows:

$$\boxed{v(t) = \int \underbrace{\mathrm{e}^{-2z\,\alpha(f)}} P(f)\, \mathrm{e}^{\imath 2\pi f (t - \frac{2z}{c})}\, \mathrm{d}f \neq p\left(t - \frac{2z}{c}\right),} \tag{U.1}$$

where the **amplitude attenuation coefficient** $\alpha(f)$ increases with frequency $|f|$.
What are the units of α? **??** Why factor of 2? **??**
Attenuation causes two primary effects.

- Signal loss (decreasing amplitude) with increasing depth z
- Pulse **dispersion** due to frequency-dependent attenuation.

Narrowband pulses

The effect of signal loss is easiest to understand for a **narrowband pulse**. We say $p(t)$ is **narrowband** if its spectrum is concentrated near $f \approx f_0$ and $f \approx -f_0$, for some center frequency f_0,

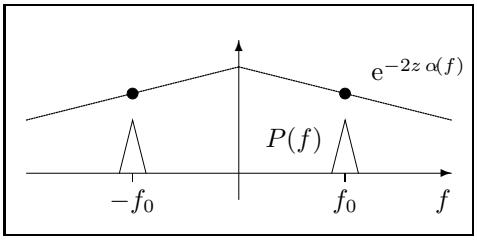

For a narrowband pulse, the following approximation to the effect of attenuation is reasonable:

$$\mathrm{e}^{-2z\,\alpha(f)}\,P(f) \approx \mathrm{e}^{-2z\,\alpha(f_0)}\,P(f). \tag{U.2}$$

Substituting that approximation into (U.1) yields

$$v(t) \approx \mathrm{e}^{-2z\,\alpha(f_0)} \int P(f)\,\mathrm{e}^{\imath 2\pi f(t-\frac{2z}{c})}\,\mathrm{d}f = \underbrace{\mathrm{e}^{-2z\,\alpha(f_0)}}\,p\left(t - \frac{2z}{c}\right). \tag{U.3}$$

In words, a narrowband pulse is simply attenuated according to the attenuation coefficient at the carrier frequency f_0; the pulse shape itself is not distorted (no dispersion). We will use this approximation throughout our discussion of ultrasound PSF.
In (U.3), the attenuation increases with range z. Therefore one usually applies **attenuation correction** to try to compensate for this loss:

$$v_{\mathrm{c}}(t) \triangleq \mathrm{e}^{2z\,\alpha(f_0)}\Big|_{z=ct/2} v(t) = \mathrm{e}^{ct\,\alpha(f_0)}\,v(t)\,. \tag{U.4}$$

What is the drawback of using narrowband pulses? They are wider in time, providing poorer range resolution.

Furthermore, for smaller wavelengths (higher frequency) there is more attenuation, so less signal, so lower SNR. This is an example of the type of **resolution-noise tradeoff** that is present in all imaging systems.

Dispersion

In practice, to provide adequate range resolution, medical ultrasound systems use fairly **wideband pulses** (*cf.* figure on U.6) that do not satisfy the narrowband approximation (U.2).

For general wideband pulses, it is difficult to simplify (U.1) to analyze the time-domain effects of frequency-dependent attenuation. Qualitatively, because different frequency components are attenuated by different amounts, the pulse shape is distorted. Multiplication by $H(f) = \mathrm{e}^{-2z\,\alpha(f)}$ in the frequency domain is equivalent to convolution with some impulse response $h(t)$ in the time domain. This convolution will spread out the pulse and the resulting distortion is called **dispersion**.

It is easiest to illustrate dispersion by evaluating (U.1) numerically, as illustrated in the following figure.

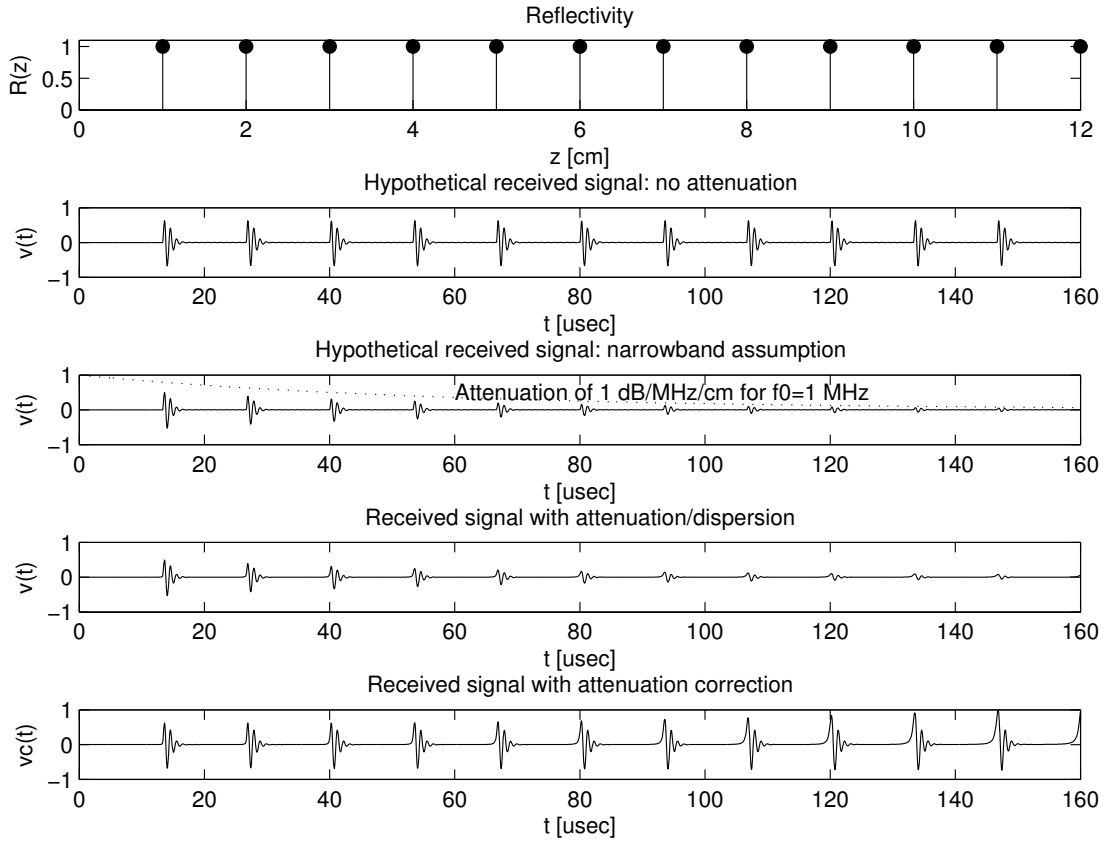

Amplitude modulated pulses

Although dispersion is challenging to analyze for general pulses, it is somewhat easier for **amplitude modulated pulses** of the form $p(t) = a(t)\cos(2\pi f_0 t)$, where $a(t)$ denotes the **envelope** of the pulse and f_0 denotes the **carrier frequency**.
By Euler's identity we can write $\cos(2\pi f_0 t) = \frac{1}{2}\mathrm{e}^{\imath 2\pi f_0 t} + \frac{1}{2}\mathrm{e}^{-\imath 2\pi f_0 t}$, and usually it is easier to analyze one of those terms at time.
Therefore, often hereafter we consider "amplitude modulated" pulses of the form $\boxed{p(t) = a(t)\,\mathrm{e}^{\imath 2\pi f_0 t}}$.

The corresponding spectrum is $P(f) = A(f - f_0)$, where $a(t) \stackrel{\mathcal{F}}{\longleftrightarrow} A(f)$.

Define the "recentered" signal $v_z(t) \triangleq v\left(t + \frac{2z}{c}\right)$. Without attenuation, we would have: $v_z(t) = p(t)$. Accounting for attenuation:

$$\begin{aligned} v_z(t) &= \int \mathrm{e}^{-2z\,\alpha(f)}\, P(f)\,\mathrm{e}^{\imath 2\pi f t}\,\mathrm{d}f = \int \mathrm{e}^{-2z\,\alpha(f)}\, A(f - f_0)\,\mathrm{e}^{\imath 2\pi f t}\,\mathrm{d}f \\ &= \mathrm{e}^{\imath 2\pi f_0 t} \int \mathrm{e}^{-2z\,\alpha(f+f_0)}\, A(f)\,\mathrm{e}^{\imath 2\pi f t}\,\mathrm{d}f = a_z(t)\,\mathrm{e}^{\imath 2\pi f_0 t}, \end{aligned}$$

by making the change of variables $f' = f - f_0$, where $\boxed{a_z(t) = d_z(t) * a(t)}$ is the envelope for a reflection from depth z accounting for attenuation,
and $d_z(t)$ is the time-domain signal ("dispersion function") with Fourier Transform $D_z(f) = \mathrm{e}^{-2z\,\alpha(f+f_0)}$.
Note $d_0(t) = \delta(t)$.
Thus the envelope of the recentered received signal is

$$|\,v_z(t)\,| = |\,a_z(t)\,| = |d_z(t) * a(t)\,|.$$

This depth-dependent blurring reduces depth spatial resolution.
One can use the above analysis to study dispersion effects (HW).

Example. Dispersion for a rect pulse envelope (which is not narrowband) is shown below.
(Each echo is normalized to have unity maximum for display.)

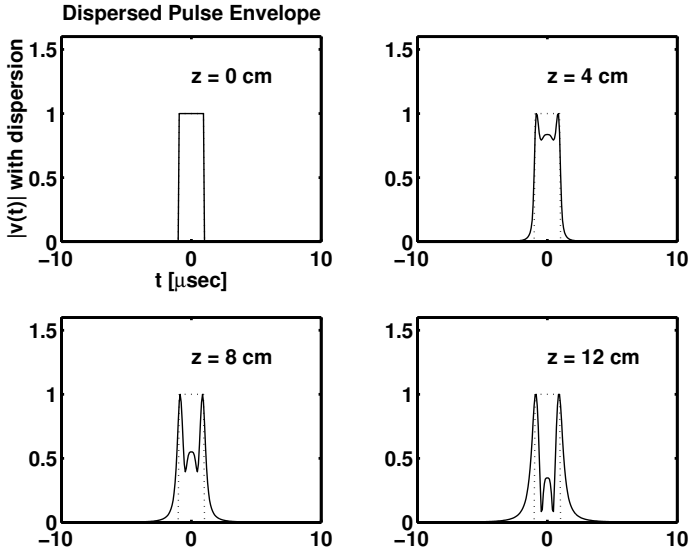

How can we reduce dispersion? **??**

Gaussian envelopes

On a log scale, attenuation is roughly linear in frequency (about 1dB/cm/MHz) over the frequency range of interest.
I.e. $\alpha(f) \approx \beta|f|$ for f between 1 and 10 MHz, where $1 \approx 20 \log_{10} \mathrm{e}^{\beta} = 20\beta \log_{10} e$, so $\beta \approx 1/(20 \log_{10} e) \approx 0.1$ MHz^{-1}cm^{-1}.

The property $\alpha(f) \approx \beta|f|$ provides an opportunity to minimize dispersion: use pulses with **Gaussian envelopes**: $A(f) = \mathrm{e}^{-w^2 f^2}$ where w is related to the time-width of the envelope.

Assuming $f_0 \gg 0$,

$$\mathrm{e}^{-2z\,\alpha(f+f_0)}\,A(f) = \mathrm{e}^{-2z\beta\cdot|f+f_0|}\,A(f) \approx \mathrm{e}^{-2z\beta\cdot(f+f_0)}\,A(f).$$

(Do not use this approximation in HW.)

With this approximation:

$$\mathrm{e}^{-2z\,\alpha(f+f_0)}\,A(f) \approx \mathrm{e}^{-2z\beta\cdot(f+f_0)}\,A(f) = \mathrm{e}^{-\left[2z\beta\cdot(f+f_0)+w^2f^2\right]}.$$

Complete the square in the exponent:

$$2z\beta\cdot(f+f_0) + w^2 f^2 = w^2\left(f^2 + 2f\frac{z\beta}{w^2}\right) + 2z\,\alpha_0 = w^2(f+f_z)^2 - w^2 f_z^2 + 2z\,\alpha_0,$$

where and $\alpha_0 = \beta f_0 = \alpha(f_0)$ is the attenuation coefficient at the carrier frequency,
and $f_z = z\beta/w^2$ is an attenuation-induced (apparent) **frequency shift**. Thus

$$\mathrm{e}^{-2z\,\alpha(f+f_0)}\,A(f) \approx \mathrm{e}^{-2z\,\alpha_0}\,A(f+f_z)\,\mathrm{e}^{(wf_z)^2}.$$

So in the time domain, for this gaussian envelope model:

$$a_z(t) = \int \mathrm{e}^{-2z\,\alpha(f+f_0)}\,A(f)\,\mathrm{e}^{\imath 2\pi f t}\,\mathrm{d}f = \mathrm{e}^{-2z\,\alpha_0}\,a(t)\,\mathrm{e}^{-\imath 2\pi f_z t}\,\mathrm{e}^{(wf_z)^2},$$

which has no dispersion, just extra gain factors that can be compensated and a phase factor that disappears with envelope detection.

So in principle, using envelopes that are approximately Gaussian is attractive.

A typical imaging transducer has a **fractional bandwidth** of about 30-50%. This means that the envelope $a(t)$ has a duration of about 2-3 periods of the carrier, *i.e.*, 2-3 wavelengths depth resolution (*cf.* earlier figure).

Summary

- Depth resolution is determined by width of acoustic pulse.
- Resolution improves as pulse becomes shorter / higher frequency.
- Attenuation also increases with increasing frequency.
- Attenuation causes signal loss and dispersion.
- Gaussian pulse envelopes are less sensitive to dispersion effects.

Notes:
- $\mathrm{e}^{-|t|} \overset{\mathcal{F}}{\longleftrightarrow} 2/(1+(2\pi f)^2)$
- See [4] for an example of more sophisticated attenuation compensation.

B-mode scan: near-field analysis

Now we begin to study the PSF of reflection-mode ultrasound imaging, specifically the brightness mode scan (**B-mode scan**).

We begin with **near-field analysis** of a mechanically scanned transducer. This analysis is quite approximate, but still the *process* is a useful preview to the more complete (but more complicated) diffraction analysis that follows. The steps are as follows.

- Derive an approximate signal model.
- Use that model to specify a (simple) image formation method.
- Relate the expression for the formed image $\hat{R}(x,y,z)$ to the ideal image $R(x,y,z)$ to analyze the PSF of the system.

Near-field signal model

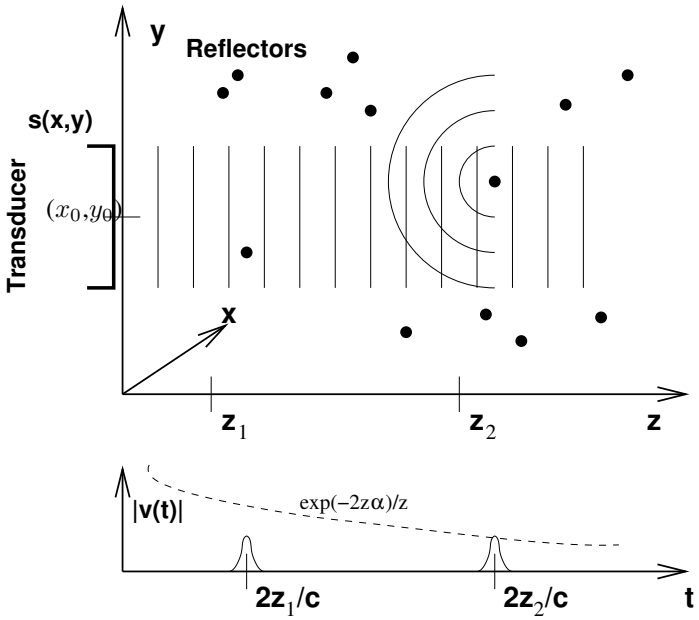

We first focus on the "near field" of a mechanically scanned transducer, illustrated above, making these simplifying assumptions.

- Single transducer element
- Face of transducer much larger than wavelength λ of propagating wave, so incident pressure approaches geometric extension of transducer face $s(x,y)$ (*e.g.*, circ or rect function). Called **piston** mode.
- Neglect diffraction spreading on transmit
- Uniform propagation velocity c
- Uniform linear attenuation coefficient α, assumed frequency independent, *i.e.*, ignoring dispersion. (Focus on lateral PSF.)
- Body consists of isotropic scatterers with scalar reflectivity $R(x,y,z)$.
  No specular reflections: structures small relative to wavelength, or large but very rough surfaces.
- Amplitude-modulated pulse $p(t) = a(t)\,\mathrm{e}^{\imath\omega_0 t}$
- Weakly reflecting medium, so ignore 2nd order and higher reflections. (See HW.)

Pressure propagation: approximate analysis

Suppose the transducer is translated to be centered at (x_0,y_0), *i.e.*, $s(x-x_0, y-y_0)$.
Let $p_{\mathrm{inc}}^{(x_0,y_0)}(x,y,z,t)$ denote the incident pressure wave that propagates in the z direction away from the transducer.
Assume that the pressure at the transducer plane ($z=0$) is:

$$p_{\mathrm{inc}}^{(x_0,y_0)}(x,y,0,t) = s(x-x_0,y-y_0)\,p(t) = s(x-x_0,y-y_0)\,a(t)\,\mathrm{e}^{\imath\omega_0 t}\,.$$

Ignoring transmit spreading, the incident pressure is a spatially truncated (due to transducer size) and attenuated pressure wave:

$$p_{\mathrm{inc}}^{(x_0,y_0)}(x,y,z,t) = \underbrace{p_{\mathrm{inc}}^{(x_0,y_0)}(x,y,0,t-z/c)}_{\text{simple propagation}}\ \underbrace{\mathrm{e}^{-\alpha z}}_{\text{attenuation}} = s(x-x_0,y-y_0)\,p(t-z/c)\,\mathrm{e}^{-\alpha z}\,.$$

We need to determine the reflected pressure $p_{\mathrm{ref}}^{(x_0,y_0)}(x,y,0,t)$ incident on the transducer. We do so by using superposition. We first find $p_{\mathrm{ref}}^{(x_0,y_0)}(x,y,0,t;x_1,y_1,z_1)$, the pressure reflected from a single ideal point reflector located at (x_1,y_1,z_1), and then compute the overall reflected pressure by **superposition** (assuming linearity, *i.e.*, small acoustic perturbations):

$$p_{\mathrm{ref}}^{(x_0,y_0)}(x,y,0,t) = \iiint R(x_1,y_1,z_1)\, p_{\mathrm{ref}}^{(x_0,y_0)}(x,y,0,t;x_1,y_1,z_1)\,\mathrm{d}x_1\,\mathrm{d}y_1\,\mathrm{d}z_1\,.$$

An ideal point reflector located at (x_1,y_1,z_1), *i.e.*, for $R(x,y,z) = \delta(x-x_1,y-y_1,z-z_1)$, would exactly reflect whatever pressure is incident at that point, and produce a wave traveling back towards the transducer. If the point reflector is sufficiently far from the transducer plane, then the spherical waves are approximately planar by the time they reach the transducer. (Admittedly this seems to be contrary to the near-field assumption.) Thus we assume:

$$p_{\mathrm{ref}}^{(x_0,y_0)}(x,y,z,t;x_1,y_1,z_1) = \underbrace{p_{\mathrm{inc}}^{(x_0,y_0)}(x_1,y_1,z_1,t+(z-z_1)/c)}_{\text{simple propagation}}\ \underbrace{\mathrm{e}^{-\alpha(z_1-z)}}_{\text{attenuation}}\ \underbrace{\frac{1}{z_1-z}}_{\text{spreading}}\,,$$

where the $1/(z_1-z)$ is due to diffraction spreading of the energy on return. In particular, back at the transducer plane ($z=0$):

$$\begin{aligned} p_{\mathrm{ref}}^{(x_0,y_0)}(x,y,0,t;x_1,y_1,z_1) &= \underbrace{p_{\mathrm{inc}}^{(x_0,y_0)}(x_1,y_1,z_1,t-z_1/c)}_{\text{simple propagation}}\ \underbrace{\mathrm{e}^{-\alpha z_1}}_{\text{attenuation}}\ \underbrace{\frac{1}{z_1}}_{\text{spreading}} \\ &= s(x_1-x_0,y_1-y_0)\,p(t-2z_1/c)\,\frac{\mathrm{e}^{-\alpha 2z_1}}{z_1}. \end{aligned}$$

Applying the superposition integral:

$$\begin{aligned} p_{\mathrm{ref}}^{(x_0,y_0)}(x,y,0,t) &= \iiint R(x_1,y_1,z_1)\, p_{\mathrm{ref}}^{(x_0,y_0)}(x,y,0,t;x_1,y_1,z_1)\,\mathrm{d}x_1\,\mathrm{d}y_1\,\mathrm{d}z_1 \\ &= \iiint R(x_1,y_1,z_1)\, s(x_1-x_0,y_1-y_0)\,p(t-2z_1/c)\,\frac{\mathrm{e}^{-\alpha 2z_1}}{z_1}\,\mathrm{d}x_1\,\mathrm{d}y_1\,\mathrm{d}z_1\,. \end{aligned} \tag{U.5}$$

The output signal from an ideal transducer would be proportional to the integral of the (reflected) pressure that impinges on its face. The constant of proportionality is unimportant for the purposes of qualitative visual display and resolution analysis. (It would affect quantitative SNR analyses.) For convenience we assume:

$$v(x_0,y_0,t) = \frac{1}{\iint s(x,y)\,\mathrm{d}x\,\mathrm{d}y} \iint s(x-x_0,y-y_0)\, p_{\mathrm{ref}}^{(x_0,y_0)}(x,y,0,t)\,\mathrm{d}x\,\mathrm{d}y,$$

where we reiterate that the received signal depends on the transducer position (x_0,y_0), because we will be moving the transducer. Under the (drastic) simplifying assumptions made above, the pressure $p_{\mathrm{ref}}^{(x_0,y_0)}(x,y,0,t)$ is independent of x,y, so by (U.5) the recorded signal is simply:

$$\begin{aligned} v(x_0,y_0,t) &= p_{\mathrm{ref}}^{(x_0,y_0)}(\cdot,\cdot,0,t) \\ &= \iiint R(x_1,y_1,z_1)\, s(x_1-x_0,y_1-y_0)\,\mathrm{e}^{\imath\omega_0(t-2z_1/c)}\, a(t-2z_1/c)\,\frac{\mathrm{e}^{-\alpha 2z_1}}{z_1}\,\mathrm{d}x_1\,\mathrm{d}y_1\,\mathrm{d}z_1 \\ \therefore\ &\boxed{v(x_0,y_0,t) \approx \frac{\mathrm{e}^{-\alpha ct}}{ct/2} \iiint R(x_1,y_1,z_1)\, s(x_1-x_0,y_1-y_0)\, a(t-2z_1/c)\,\mathrm{d}x_1\,\mathrm{d}y_1\,\mathrm{d}z_1,} \end{aligned} \tag{U.6}$$

where we assume the pulse envelope is narrow, *i.e.*, $a(t) \approx \delta(t)$.

(See picture above for sketch of signal. Note the distance-dependent loss $\mathrm{e}^{-\alpha 2z_1}/z_1$.)

To help interpret (U.6), consider the most "idealized" case where $s(x,y) = \delta_2(x,y)$ (tiny transducer) and $a(t) = \delta(t)$ (short pulse). Then by the Dirac impulse sifting property:

$$v(x_0,y_0,t) = R(x_0,y_0,z_1)\frac{\mathrm{e}^{-\alpha 2z_1}}{z_1}\bigg|_{z_1=ct/2}\,. \tag{U.7}$$

Near-field image formation

How do we perform **image formation**, *i.e.*, form an image $\hat{R}(x,y,z)$ from the received signal(s) $v(x_0,y_0,t)$?

Frequently this question is answered first by considering very idealized signal models such as (U.6) or (U.7).
In light of the ideal relationship (U.7), we must:
- relate time to distance using $z = ct/2$ or $t = 2z/c$, and
- try to compensate for the signal loss due to attenuation and spreading by multiplying by a suitable **gain** term. (In practical systems, the gain as a function of depth is adjusted both automatically and by manual sliders.)

Rearranging (U.7) leads to the following very simple image formation relationship for estimating reflectivity:

$$\boxed{\hat{R}(x,y,z) \triangleq \underbrace{\frac{ct}{2} \mathrm{e}^{ct\,\alpha}}_{\text{gain}} |v(x,y,t)| \Big|_{t=\frac{2z}{c}}.} \tag{U.8}$$

This time/depth-dependent gain is called **attenuation correction**.
Note that we must translate (scan) the transducer to every x, y position where we want to observe $R(x,y,z)$.

Near-field PSF (Geometric PSF)

How does our estimated image $\hat{R}(x,y,z)$ relate to the true reflectivity $R(x,y,z)$?
If we substituted the extremely approximate signal model (U.7) into the image formation expression (U.8) we would conclude erroneously that $\hat{R}(x,y,z) = R(x,y,z)$.
Although simple measurement models are often adequate for designing simple image formation methods, when we want to understand the limitations of such methods usually we must analyze more accurate models.

Substituting the (somewhat more accurate) signal model (U.6) into the image formation expression (U.8) yields

$$\begin{aligned}
\hat{R}(x,y,z) &= \left| \iiint R(x_1,y_1,z_1)\, s(x_1-x, y_1-y)\, a(2z/c - 2z_1/c)\, \mathrm{d}x_1\, \mathrm{d}y_1\, \mathrm{d}z_1 \right| \\
&\approx \iiint R(x_1,y_1,z_1)\, s(x_1-x, y_1-y)\, a\left(\frac{2}{c}(z-z_1)\right) \mathrm{d}x_1\, \mathrm{d}y_1\, \mathrm{d}z_1,
\end{aligned}$$

where the approximation is reasonable provided the pulse is sufficiently narrow.

Under all of the (unrealistic) simplifying assumptions we have made, the PSF has turned out to be space invariant, and the final superposition integral simplifies to the form of a convolution:

$$\boxed{\hat{R}(x,y,z) \approx R(x,y,z) \mathbin{***} h_{\mathrm{Geometric}}(x,y,z),}$$

where the "geometric" PSF is given by:

$$\boxed{h_{\mathrm{Geometric}}(x,y,z) = s(-x,-y)\, a\left(\frac{2z}{c}\right).}$$

This PSF is **separable** between the transverse plane (x,y) and range z.

Now we can address how system design affects the imaging PSF.
- The lateral or transverse spatial resolution is determined by the transducer shape.
- The depth resolution is determined by the pulse envelope.

Example. For a 4mm square transducer, the PSF is 4mm wide in the x, y plane.
A typical pulse envelope has a duration of 2-3 periods of its carrier, *i.e.*, its width is roughly $\Delta_t = 2/f_0$, so the width of $a(2z/c)$ is roughly $\Delta_z = c\Delta_t/2 = c/f_0 = \lambda$. If $c = 1500$ m/s and $f_0 = 1$ MHz, then the wavelength is $\lambda = c/f_0 = 1.5$ mm.

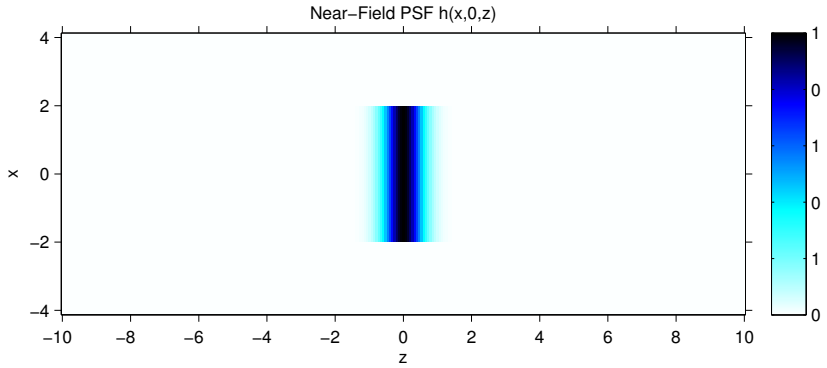

So we can improve the **depth resolution** by using a higher carrier frequency f_0. What is the tradeoff? More attenuation! So we have a **resolution-noise tradeoff**. Such tradeoffs exist in all imaging modalities.

Although this simplified analysis suggests that the ideal transducer would be very small, the analysis assumed at the outset that the transducer is large (relative to the wavelength)! So it is premature to draw definitive conclusions about designing transducer size.

However, when we properly account for diffraction, we will see that the PSF h is *not* space invariant, so it will *not be possible to write the superposition integral as a convolution*. Virtually all of the triple convolutions in Ch. 9 and Ch. 10 of Macovski are incorrect. But the superposition integrals that precede the triple convolutions are fine.

Even though the PSF will vary with depth z, it is still quite interpretable.

Using more detailed analysis, one can show that the geometric model is reasonable for $z < D^2/2\lambda$ for a square transducer or $z < D^2/4\lambda$ for a circular transducer [3, p 333]. The **Fresnel region** extends from that point out to $z = D^2/\lambda$. Beyond that is the **Fraunhofer region** or **far field**.

A-mode scan

If the transducer is held at a fixed position (x_0,y_0) and a plot of reflectivity vs depth, *i.e.*, $\hat{R}(x_0, y_0, z)$ vs z, is made, then this is called an **A-mode scan**.

B-mode scan (Brightness) (Usual mode)

- Translate transducer (laterally) to different location (x, y) (usually fixing x or y and translating w.r.t. the other)
  Typically x-motion by mechanical translation of transducer, y-motion by manual selection of operator.
- Form lines of image from different positions.
- Assume transducer motion slow relative to pulse travel.
- Everything shift-invariant w.r.t. x and y due to scanning.

What if sound velocity c is not constant (*i.e.*, varies in different tissue types)?

Depth variance of PSF

It would be nice if in general for an A-mode scan we could find a PSF $h_{\mathrm{psf}}(x,y,z)$ for which

$$|v_{\mathrm{c}}(t)| = |(R \ast\!\ast\!\ast\, h_{\mathrm{psf}})(0,0,tc/2)|$$

so that we can form a line of the image by:

$$\hat{R}(0,0,z) = |v_{\mathrm{c}}(2z/c)| = |(R \ast\!\ast\!\ast\, h_{\mathrm{psf}})(0,0,z)| \,.$$

Unfortunately, for propagation models that are more realistic than those we used above, the PSF is *depth-variant* (varies with z), so we *cannot* express $v_{\mathrm{c}}(t)$ or $\hat{R}$ as a 3D convolution like above.
Nearly all equations in Ch. 9 and 10 of Macovski containing $\ast\!\ast\!\ast$ are incorrect! The integral equations are fine.
We will settle for describing the system function through integrals like the following:

$$\boxed{\hat{R}(0,0,z) = \left| \iiint R(x_1,y_1,z_1)\, \mathrm{e}^{\imath k 2 r_1}\, b^2(x_1,y_1,z_1)\, a\left(\frac{2}{c}(z-z_1)\right) \mathrm{d}x_1\, \mathrm{d}y_1\, \mathrm{d}z_1 \right|.}$$

- $b(x,y,z)$ determines primarily the **lateral resolution** at any depth z and varies slowly with z. It is called the **beam pattern**.
- Both the transmit and receive operations have an associated beam pattern.
  The "overall" beam pattern is the **product** of the **transmit beam pattern** and the **receive beam pattern**.
  For a single transducer, these transmit and receive beam patterns are identical, so the PSF contains the squared term b^2.
- $a\big(\frac{2}{c}(z-z_1)\big)$ determines primarily the **depth resolution**,
- $r_1 = \sqrt{x_1^2 + y_1^2 + z_1^2}$
- $\mathrm{e}^{\imath k 2 r_1}$ is an unavoidable (and unfortunate) phase term, where $k = 2\pi/\lambda$ is the wave number.
  (Its presence causes destructive interference aka speckle.)

If we image by translating the transducer, then everything will be translation invariant w.r.t. x and y, so in particular:

$$\begin{aligned} \hat{R}(x,y,z) &= \left| \iiint R(x_1,y_1,z_1)\, \mathrm{e}^{\imath 2 k r_1}\, b^2(x_1-x,y_1-y,z_1)\, a\left(\frac{2}{c}(z-z_1)\right) \mathrm{d}x_1\, \mathrm{d}y_1\, \mathrm{d}z_1 \right| \\ &= \left| \iiint R(x_1,y_1,z_1)\, \mathrm{e}^{\imath 2 k r_1}\, h(x-x_1,y-y_1,z-z_1;z_1)\, \mathrm{d}x_1\, \mathrm{d}y_1\, \mathrm{d}z_1 \right|, \end{aligned}$$

where

$$\boxed{h(x,y,z;z_1) = b^2(-x,-y,z_1)\, a\left(\frac{2}{c}z\right).}$$

Due to the explicit dependence of the PSF on depth z_1, the PSF is shift variant or, in this case, **depth dependent**.

Mathematical interpretation: if $R(x,y,z) = \delta(x-x_1', y-y_1', z-z_1')$, then

$$\hat{R}(x,y,z) = b^2(x_1'-x, y_1'-y, z_1')\, a\left(\frac{2}{c}(z-z_1')\right),$$

which is the lateral PSF $b^2(\cdot,\cdot,z_1')$ at depth z_1' translated to (x_1,y_1), and blurred out in depth z by the pulse $a\big(\frac{2}{c}\cdot\big)$.

Physical interpretation: the PSF $h(x,y,z;z_1)$ describes how much the reflectivity from point (x,y,z_1) will contaminate our estimate of reflectivity at $(0,0,z)$.

Goals:
- Find b, interpret, and simplify
- Study how b varies with transducer size/shape.

Final form appears in (9.38):

$$b_{\mathrm{Fraunhofer}}(\theta) = \frac{\cos\theta}{\lambda} S_X\left(\frac{\sin\theta}{\lambda}\right).$$

Intermediate assumptions along the way are important to understand to see why in practice (and in the project) not everything agrees with these predictions.

Mostly follow Macovski notation, filling in some details, and avoiding potentially ambiguous notation $f(t) \cdot g(t) * h(t)$.

A-mode scan: Diffraction analysis

Diffraction: "any deviation of light rays from rectilinear paths which cannot be interpreted as reflection or refraction."

Why diffraction? Goal: more accurate PSF, because in reality wavelength fairly large relative to aperture.
($f_0 = 1.5$ MHz, $c = 1500$ m/s, $\lambda = f_0/c = 1$mm) (AM Radio: 540KHz to 1.6MHz)
Major factor in determining spatial resolution is diffraction spreading. References: [5], [6].

Geometry

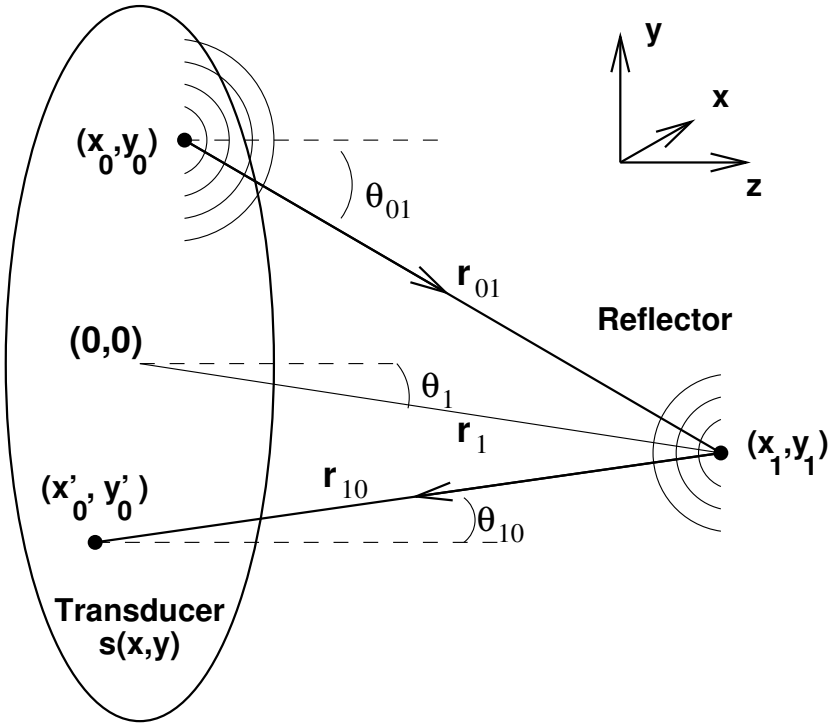

Transducer defines $(x, y, 0)$ plane. Define: $P_0 \triangleq (x_0, y_0, 0)$, $P_0' \triangleq (x_0', y_0', 0)$, $P_1 \triangleq (x_1, y_1, z_1)$.
Shorthand for radial distances:

$$r_{01} = \|P_0 - P_1\| = \|(x_0, y_0, 0) - (x_1, y_1, z_1)\| = \sqrt{(x_1 - x_0)^2 + (y_1 - y_0)^2 + z_1^2}.$$

Similarly define $r_{10} = \|P_1 - P_0'\|$ and $r_1 = \|P_1\|$.

Later we will assume that P_1 is sufficiently far from the transducer (relative to transducer size) that

$$\begin{aligned} \cos\theta_{01} &\approx \cos\theta_{10} \approx \cos\theta_1 = z_1/r_1 \\ r_{01} &\approx r_{10} \approx r_1. \end{aligned}$$

The latter approximation applies *only* within functions that vary slowly with r, like $1/r_{01}$, but *not* in terms like $\mathrm{e}^{\imath k r_{01}}$.

Superposition

The main ingredient of diffraction analysis is the **Huygens-Fresnel Principle**: superposition!
Pressure at P_1 is superposition of contributions from each point on transducer, where each point can be thought of as a point source emitting a spherical wave.

Superposition requires that we assume **linearity** of the medium, which means the pressure perturbations must be sufficiently small. Modern ultrasound systems include **harmonic imaging** modes where nonlinear effects are exploited, not considered here.

Monochromatic case

Start with **monochromatic** wave (called **continuous-wave diffraction**):

$$u(P,t) = U_a(P)\cos(2\pi f t + \phi(P)) = \text{Real}[U(P)\,\mathrm{e}^{-\imath 2\pi f t}] \quad \text{where} \quad U(P) = U_a(P)\,\mathrm{e}^{-\imath\phi(P)}$$

is complex phasor, and position: $P = (x, y, z)$.
Note everywhere the wave (pressure) is oscillating at the same frequency, only difference is amplitude and phase.

Rayleigh-Sommerfeld Theory

Using:
- linear wave equation
- Helmholz equation: $(\nabla^2 + k^2)U = 0$
- linearity and superposition
- Green's theorem
- ...

Goodman [5], shows that:

$$U(P_1) = \frac{1}{\imath\lambda}\iint_\Sigma U(P_0)\frac{\cos\theta_{01}}{r_{01}}\,\mathrm{e}^{\imath k r_{01}}\,\mathrm{d}x_0\,\mathrm{d}y_0 = \iint_\Sigma h(P_1,P_0)U(P_0)\,\mathrm{d}x_0\,\mathrm{d}y_0$$

for $r_{01} \gg \lambda$, where the "point spread function" for the phasor $U(P)$ is

$$h(P_1,P_0) = \frac{1}{\imath\lambda}\frac{\cos\theta_{01}}{r_{01}}\,\mathrm{e}^{\imath k r_{01}}\,.$$

The **wavenumber** k is defined as: $\boxed{k = \omega_0/c = 2\pi/\lambda.}$
Physical interpretation of above diffraction integral:
- Σ means integrate over the transducer (or transducer plane).
- $\cos\theta_{01}$ is obliquity factor (later assumed $\approx \cos\theta_1$).
- $1/r_{01}$ is the $1/r$ falloff of amplitude (conservation of energy on sphere with surface area proportional to r^2).
- $\mathrm{e}^{\imath k r_{01}} = \mathrm{e}^{\imath\omega_0(r_{01}/c)}$ is phase change due to propagation over distance r_{01} (time delay of r_{01}/c).

The **reciprocity theorem of Helmholz** states that $h(P_0,P_1) = h(P_1,P_0)$.

Propagation is shift-invariant; translating the entire coordinate system has no effect on wave propagation.

Polychromatic case

By Fourier decomposition, Goodman [5] shows that, $\boxed{\text{assuming } r_{01} \gg \lambda,}$ for **polychromatic** waves, the pressure at point P_1 relates to the pressure at the transducer plane as follows:

$$\boxed{u(P_1,t) = \iint_\Sigma \frac{\cos\theta_{01}}{r_{01}}\frac{1}{2\pi c}\frac{\mathrm{d}}{\mathrm{d}t}\,u\Big(P_0, t - \frac{r_{01}}{c}\Big)\,\mathrm{d}x_0\,\mathrm{d}y_0\,.} \qquad \text{(Goodman:3-33)}$$

This is the starting point for our analysis.
For $\frac{\mathrm{d}}{\mathrm{d}t}$, *cf.* shaking a rope: large slow displacement vs small fast shake.
Note that we are *ignoring attenuation* to focus on diffraction effects.
We use "u" not "p" for pressure here, consistent with Goodman / Macovski, because we use P for points and $p(t)$ for pulse.

Preview

Our strategy now will be to combine (Goodman:3-33) with the principles of **superposition** and **reciprocity**, by analogy with the preceding near-field analysis. One approach is to use superposition first, and then make simplifying approximations [8]. An alternative derivation considered here is to first simplify (Goodman:3-33) by making several approximations, and *then* use superposition and reciprocity.

Insonification ("filling the volume with acoustic wavelets")

If the transducer is pulsed coherently over its face (**piston mode**) with output pressure $p_0(t)$, then at the transducer plane:

$$\boxed{u(P_0, t) = s(x_0, y_0)\, p_0(t),} \tag{9.15}$$

i.e., at plane $z = 0$ the pressure is zero everywhere except over the transducer face.

Narrowband approximation (for amplitude modulated pulses)

Assume we use an amplitude modulated pulse:

$$\boxed{p_0(t) = a_0(t)\, \mathrm{e}^{-\imath\omega_0 t}\,,}$$

where $a_0(t)$ includes the transducer's impulse response. In practice, one can determine experimentally the pulse envelope $a_0(t)$ using wire phantoms.

From (Goodman:3-33), we see we will need derivatives of the pressure. These expressions simplify considerably if we assume that the pulse is **narrowband**. In short, a narrowband amplitude modulated pulse satisfies the following approximation:

$$\boxed{\frac{\mathrm{d}}{\mathrm{d}t}\, a_0(t)\, \mathrm{e}^{-\imath\omega_0 t} \approx -\imath\omega_0\, a_0(t)\, \mathrm{e}^{-\imath\omega_0 t}\,,} \textit{ i.e., } \boxed{\frac{\mathrm{d}}{\mathrm{d}t}\, p_0(t) \approx -\imath\omega_0\, p_0(t)\,.}$$

In particular, because $c = \lambda f_0$, under the narrowband approximation the time derivative of the input pressure is:

$$\boxed{\frac{1}{2\pi c}\frac{\mathrm{d}}{\mathrm{d}t} u(P_0, t) \approx -\imath\frac{1}{\lambda} u(P_0, t) = -\imath\frac{1}{\lambda}\, s(x_0, y_0)\, p_0(t)\,.} \tag{U.11}$$

To explore the narrowband approximation in the time domain, use the product rule:

$$p_1(t) \triangleq \frac{1}{2\pi f_0}\frac{\mathrm{d}}{\mathrm{d}t}\, p_0(t) = a_1(t)\, \mathrm{e}^{-\imath\omega_0 t}\,, \quad \text{where} \quad a_1(t) \triangleq \frac{1}{2\pi f_0}\, \dot{a}_0(t) - \imath\, a_0(t)\,.$$

One way of defining a **narrowband** pulse is to require that $|\dot{a}_0(t)| \ll f_0$, in which case $a_1(t) \approx -\imath\, a_0(t)$ so $p_1(t) \approx -\imath\, p_0(t)$.

More typically, we define a **narrowband** pulse in terms of its spectrum, namely that the width of the frequency response of $a_0(t)$ is much smaller than the carrier frequency f_0. Because $p_0(t) = a_0(t)\, \mathrm{e}^{-\imath\omega_0 t}$, in the frequency domain $P_0(f) = A_0(f + f_0)$. By the derivative property of Fourier transforms:

$$p_1(t) = \frac{1}{2\pi f_0}\frac{\mathrm{d}}{\mathrm{d}t}\, p_0(t) \overset{\mathcal{F}}{\longleftrightarrow} P_1(f) = \frac{1}{2\pi f_0}(\imath 2\pi f) P_0(f) = \frac{\imath f}{f_0} A_0(f + f_0) \approx \frac{\imath(-f_0)}{f_0} A_0(f + f_0) = -\imath A_0(f + f_0) = -\imath P_0(f).$$

Thus, taking the inverse FT: $p_1(t) = \frac{1}{2\pi f_0}\frac{\mathrm{d}}{\mathrm{d}t}\, p_0(t) \approx -\imath\, p_0(t)$.

Simplified incident pressure

At this point we also assume that $\boxed{\cos\theta_{01} \approx \cos\theta_{10} \approx \cos\theta_1}$ and $\boxed{r_{01} \approx r_{10} \approx r_1,}$ within terms that vary slowly with those quantities. Combining (Goodman:3-33) with (U.11) leads to the following approximation for the incident pressure:

$$\begin{aligned} u(P_1, t) &\approx -\imath\frac{\cos\theta_1}{\lambda r_1} \iint u\Big(P_0, t - \frac{r_{01}}{c}\Big)\, \mathrm{d}x_0\, \mathrm{d}y_0, \qquad r_{01} = \sqrt{(x_0 - x_1)^2 + (y_0 - y_1)^2 + (0 - z_1)^2} \\ &= -\imath\frac{\cos\theta_1}{\lambda r_1}\, \mathrm{e}^{-\imath\omega_0 t} \iint s(x_0, y_0)\, \mathrm{e}^{\imath k r_{01}}\, a_0\Big(t - \frac{r_{01}}{c}\Big)\, \mathrm{d}x_0\, \mathrm{d}y_0\,. \end{aligned} \tag{U.12}$$

Steady-state approximation (for narrowband pulse)

The **steady-state** or **plane wave** approximation is:

$$\boxed{a_0\Big(t - \frac{r_{01}}{c}\Big) \approx a_0\Big(t - \frac{r_1}{c}\Big)\,.} \tag{9.21}$$

- Assumes envelope of waveform emitted from all parts of the transducer arrive at point P_1 at about same time.
- Need pulse-width $\tau \gg D^2/(8r_1c)$, where D is transducer "diameter."
  If $\tau = 3/f_0$, then need $r_1 \gg D^2/(32\lambda) \approx 3$ mm if $D = 10$ mm and $\lambda = 1$ mm.
- Accurate for long pulses (narrowband). But short pulses give better depth resolution...
- Poor approximation for large transducers or small depths z_1.
- Makes lateral resolution determined by relative phases over transducer, not by pulse envelope.

Applying the **steady-state** or **plane wave** approximation (9.21) to (U.12) yields the final incident pressure field approximation:

$$u(P_1,t) \approx -\imath\,\mathrm{e}^{-\imath\omega_0 t}\,\frac{\cos\theta_1}{\lambda r_1}\left(\iint s(x_0,y_0)\,\mathrm{e}^{\imath k r_{01}}\,\mathrm{d}x_0\,\mathrm{d}y_0\right) a_0\Big(t - \frac{r_1}{c}\Big)\,.$$

If point P_1 has reflectivity $R(P_1)$, then by **reciprocity** the contribution of that (infinitesimal) point to the (differential) pressure reflected back to transducer point P_0' is (applying again the narrow band and steady-state approximations):

$$\begin{aligned}
\tilde{u}(P_0',t;P_1) &= R(P_1)\frac{\cos\theta_{10}}{\lambda r_{10}}\frac{1}{2\pi c}\frac{\mathrm{d}}{\mathrm{d}t}\,u\Big(P_1, t - \frac{r_{10}}{c}\Big) \\
&\approx R(P_1)\frac{\cos\theta_1}{\lambda r_1}\left(\frac{-\imath}{\lambda}\right) u\Big(P_1, t - \frac{r_{10}}{c}\Big) \text{ [using narrowband approximation]} \\
&\approx R(P_1)\frac{1}{\lambda}\left(\frac{\cos\theta_1}{\lambda r_1}\right)^2 \mathrm{e}^{-\imath\omega_0 t}\left(\iint s(x_0,y_0)\,\mathrm{e}^{\imath k r_{01}}\,\mathrm{d}x_0\,\mathrm{d}y_0\right)\mathrm{e}^{\imath k r_{10}}\,a\Big(t - \frac{2r_1}{c}\Big), \text{ [using ss]}
\end{aligned}$$

where $a(t) \triangleq (-\imath)^2\,a_0(t)$. Now apply **superposition** over all possible reflectors in 3D object space:

$$\begin{aligned}
u(P_0';t) &= \iiint \tilde{u}(P_0',t;P_1)\,\mathrm{d}P_1 \\
&\approx \frac{1}{\lambda}\,\mathrm{e}^{-\imath\omega_0 t}\iiint R(P_1)\left(\frac{\cos\theta_1}{\lambda r_1}\right)^2\left(\iint s(x_0,y_0)\,\mathrm{e}^{\imath k r_{01}}\,\mathrm{d}x_0\,\mathrm{d}y_0\right)\mathrm{e}^{\imath k r_{10}}\,a\Big(t - \frac{2r_1}{c}\Big)\,\mathrm{d}P_1\,.
\end{aligned}$$

Signal model

Assuming transducer linearity the output **signal** is (proportional to) the integral of the reflected pressure over the transducer:

$$\begin{aligned}
v(t) &= K\lambda\iint s(x_0',y_0')\,u(P_0';t)\,\mathrm{d}x_0'\,\mathrm{d}y_0' \\
&\approx K\,\mathrm{e}^{-\imath\omega_0 t}\iint s(x_0',y_0')\left[\iiint R(P_1)\left(\frac{\cos\theta_1}{\lambda r_1}\right)^2\iint s(x_0,y_0)\,\mathrm{e}^{\imath k r_{01}}\,\mathrm{d}x_0\,\mathrm{d}y_0\,\mathrm{e}^{\imath k r_{10}}\,a\Big(t - \frac{2r_1}{c}\Big)\,\mathrm{d}P_1\right]\mathrm{d}x_0'\,\mathrm{d}y_0' \\
&= K\,\mathrm{e}^{-\imath\omega_0 t}\iiint R(P_1)\left[\left(\frac{\cos\theta_1}{\lambda r_1}\right)^2\iint s(x_0',y_0')\,\mathrm{e}^{\imath k r_{10}}\,\mathrm{d}x_0'\,\mathrm{d}y_0'\iint s(x_0,y_0)\,\mathrm{e}^{\imath k r_{01}}\,\mathrm{d}x_0\,\mathrm{d}y_0\,a\Big(t - \frac{2r_1}{c}\Big)\,\mathrm{d}P_1\right]
\end{aligned}$$

- Inner: contributions from transducer point P_0 incident on volume point P_1.
- Middle: contributions from volume point P_1 reflected back to transducer point P_0'.
- Outer: integrate over transducer face for output voltage.

Simplifying yields the following **ultrasound signal equation**:

$$\boxed{v(t) \approx K \, \mathrm{e}^{-\imath \omega_0 t} \iiint R(P_1) \left(\frac{\lambda}{r_1} \right)^2 \mathrm{e}^{\imath k 2 r_1} \, b^2_{\mathrm{Narrowband}}(x_1, y_1, z_1) \, a\left(t - \frac{2 r_1}{c} \right) \mathrm{d}P_1,} \tag{U.14}$$

where we define the (unitless) **beam pattern** by

$$\boxed{b_{\mathrm{Narrowband}}(x_1, y_1, z_1) \triangleq \frac{\cos \theta_1}{\lambda^2} \iint s(x_0, y_0) \, \mathrm{e}^{\imath k (r_{01} - r_1)} \, \mathrm{d}x_0 \, \mathrm{d}y_0 \, .} \tag{U.15}$$

The expression (U.15) is suitable for numerical evaluation of transducer designs, but for intuition we want to simplify $b_{\mathrm{Narrowband}}$.

What would the ideal beam pattern be? Perhaps $b(x, y, z) = s(x, y)$, as in the geometric near-field analysis.

Image formation

The above analysis was for the transducer centered at $(0, 0)$. Based on our earlier near-field geometric analysis, and the gain corrections suggested by the signal equation above, the natural estimate of reflectivity is:

$$\begin{aligned}
\hat{R}(0,0,z) &\triangleq \underbrace{\frac{1}{K} \left(\frac{z}{\lambda} \right)^2}_{\text{gain}} \left| v\left(\frac{2z}{c} \right) \right| \\
&\approx \left| \iiint R(P_1) \, \mathrm{e}^{\imath k 2 r_1} \, b^2_{\mathrm{Narrowband}}(x_1, y_1, z_1) \, a\left(2 \frac{z - r_1}{c} \right) \mathrm{d}P_1 \right| \\
&= \left| \iiint R(P_1) \, h(0, 0, z; P_1) \, \mathrm{d}P_1 \right|,
\end{aligned} \tag{U.16}$$

where the (space varying) PSF is:

$$\boxed{h(x, y, z; P_1) \triangleq \underbrace{\mathrm{e}^{\imath k 2 r_1}}_{\text{speckle}} \underbrace{b^2_{\mathrm{Narrowband}}(x_1 - x, y_1 - y, z_1)}_{\text{lateral}} \underbrace{a\left(2 \frac{z - r_1}{c} \right)}_{\text{depth, range}}.}$$

Above we have included x, y in the PSF for generality assuming B-mode scanning. For A-mode, $x = y = 0$.

Note that $h(\cdot)$ depends on z_1, not $z - z_1$, revealing the **depth dependence** of the PSF, so it is not a convolution, even if we make the approximation $z - r_1 \approx z - z_1$ in the range term.

The phase modulation $\mathrm{e}^{\imath k 2 r_1}$ contributes to **speckle**: destructive interference of reflections from different depths.
Because $2kr = 2\pi r / (\lambda / 2)$, this term wraps around 2π every half wavelength.
If the wavelength λ is 1 mm, then this term wraps 2π in phase every 0.5 mm!

To interpret the PSF, we would like to simplify its expression, particularly the beam pattern part.

Here we needed z^2 **gain** compensation because we accounted for diffraction **spreading** in both directions.
In practice we would need additional gain to compensate for **attenuation**.

Paraxial approximation

Near the axis, $\cos\theta_1 \approx 1$, so

$$b_{\text{Narrowband}}(x_1, y_1, z_1) = \frac{\cos\theta_1}{\lambda^2} \iint s(x_0, y_0)\, \mathrm{e}^{\imath k(r_{01} - r_1)}\, \mathrm{d}x_0\, \mathrm{d}y_0 \approx b_{\text{Paraxial}}(x_1, y_1, z_1),$$

where we define

$$b_{\text{Paraxial}}(x_1, y_1, z_1) \triangleq \frac{1}{\lambda^2} \iint s(x_0, y_0)\, \mathrm{e}^{\imath k(r_{01} - r_1)}\, \mathrm{d}x_0\, \mathrm{d}y_0 = \left(s(x,y) ** \frac{1}{\lambda^2}\, \mathrm{e}^{\imath k \sqrt{x^2 + y^2 + z_1^2}} \right) \mathrm{e}^{-\imath k r_1},$$

where the 2D convolution is over x and y. Convolution with such an exponential term is hard and non-intuitive. Thus we want to further simplify b_{Paraxial} and/or $b_{\text{Narrowband}}$.

Fresnel approximation in Cartesian coordinates

To simplify (U.15), we need to make approximations to the exponent r_{01}. Consider a Taylor series approximation:

$$r_{01} = \sqrt{(x_1 - x_0)^2 + (y_1 - y_0)^2 + z_1^2} = z_1 \sqrt{1 + \frac{(x_1 - x_0)^2 + (y_1 - y_0)^2}{z_1^2}} \approx z_1 + \frac{(x_1 - x_0)^2 + (y_1 - y_0)^2}{2 z_1}$$

because $\sqrt{1+t} \approx 1 + t/2 - t^2/8$ for small t.

To drop 2nd-order term, need $k z_1 t^2 / 8 \ll 1$ for $t = \max\left\{(x_1 - x_0)^2 + (y_1 - y_0)^2\right\} / z_1^2 = (r_1 - r_0)^2 / z_1^2 = r_{\max}^2 / z_1^2$.
Thus need $z_1^3 \gg k r_{\max}^4 / 8 = r_{\max}^4 \pi / (4\lambda) \approx r_{\max}^4 / \lambda$ or $z_1 \gg r_{\max} \sqrt[3]{r_{\max}/\lambda}$.

Combining all of the above approximations:

$$\begin{aligned} b_{\text{Paraxial}}(x,y,z) &\approx \mathrm{e}^{\imath k(z - r_1)}\, b_{\text{Fresnel}}(x,y,z) \\ b_{\text{Fresnel}}(x,y,z) &\triangleq \frac{1}{\lambda^2} \iint s(x_0, y_0) \exp\left(\imath \frac{k}{2z} \left[(x - x_0)^2 + (y - y_0)^2 \right] \right) \mathrm{d}x_0\, \mathrm{d}y_0, \end{aligned} \tag{U.17}$$

$$\boxed{b_{\text{Fresnel}}(x,y,z) = s(x,y) ** \frac{1}{\lambda^2} \exp\left(\imath \frac{k}{2z} [x^2 + y^2] \right).}$$

Applying this approximation to (U.16), the gain-compensated reflectivity estimate is:

$$\hat{R}(0,0,z) \approx \left| \iiint R(x_1, y_1, z_1)\, \mathrm{e}^{\imath 2 k z_1}\, b_{\text{Fresnel}}^2(x_1, y_1, z_1)\, a\left(\frac{2}{c}(z - z_1) \right) \mathrm{d}x_1\, \mathrm{d}y_1\, \mathrm{d}z_1 \right|.$$

This *cannot* be written as a 3D convolution! (Because the lateral response b_{Fresnel} depends on z, see figures below.)

b_{Fresnel} still messy due to convolution with complex exponential with quadratic phase. (Hence no pictures yet...)

Focusing preview

$$\begin{aligned} b_{\text{Fresnel}}(x,y,z) &= \frac{1}{\lambda^2} \iint s(x_0, y_0) \exp\left(\imath \frac{k}{2z} [(x - x_0)^2 + (y - y_0)^2] \right) \mathrm{d}x_0\, \mathrm{d}y_0 \\ &= \exp\left(\imath \frac{k}{2z} [x^2 + y^2] \right) \frac{1}{\lambda^2} \iint s(x_0, y_0) \exp\left(\imath \frac{k}{2z} [x_0^2 + y_0^2] \right) \exp\left(-\imath \frac{2\pi}{\lambda z} [x x_0 + y y_0] \right) \mathrm{d}x_0\, \mathrm{d}y_0 \\ &= \exp\left(\imath \frac{k}{2z} [x^2 + y^2] \right) \frac{1}{\lambda^2} \mathcal{F}\left[s(x,y) \exp\left(\imath \frac{k}{2z} [x^2 + y^2] \right) \right] \left(\frac{x}{\lambda z}, \frac{y}{\lambda z} \right). \end{aligned}$$

To cancel phase term inside Fourier transform, use spherical (acoustic) lens of radius R having thickness proportional to

$$\sqrt{1 - \frac{x^2 + y^2}{R}} \approx 1 - \frac{x^2 + y^2}{2R}.$$

Fraunhofer approximation in Cartesian coordinates

We can rewrite the Fresnel approximation to the beam pattern (U.17) as follows::

$$\begin{aligned} b_{\text{Fresnel}}(x,y,z) &= \frac{1}{\lambda^2} \iint s(x_0,y_0) \exp\left(\imath \frac{k}{2z} [(x-x_0)^2 + (y-y_0)^2] \right) \mathrm{d}x_0 \, \mathrm{d}y_0 \\ &= \mathrm{e}^{\imath k r^2/(2z)} \frac{1}{\lambda^2} \iint s(x_0,y_0) \, \mathrm{e}^{\imath k r_0^2/(2z)} \exp\left(-\imath \frac{k}{z} [x x_0 + y y_0] \right) \mathrm{d}x_0 \, \mathrm{d}y_0, \end{aligned} \tag{9.38}$$

where $r^2 \triangleq x^2 + y^2$ and $r_0^2 \triangleq x_0^2 + y_0^2$.

Ignoring the inner phase term $\mathrm{e}^{\imath k r_0^2/(2z)}$ in (9.38) leads to the **Fraunhofer approximation** to the **beam pattern**:

$$\begin{aligned} b_{\text{Fresnel}}(x,y,z) &\approx \mathrm{e}^{\imath k r^2/(2z)} \, b_{\text{Fraunhofer}}(x,y,z) \\ b_{\text{Fraunhofer}}(x,y,z) &= \frac{1}{\lambda^2} \iint s(x_0,y_0) \exp\left(-\imath \frac{2\pi}{\lambda z} [x x_0 + y y_0] \right) \mathrm{d}x_0 \, \mathrm{d}y_0, \end{aligned}$$

$$\boxed{b_{\text{Fraunhofer}}(x,y,z) = \frac{1}{\lambda^2} S\Big(\frac{x}{\lambda z}, \frac{y}{\lambda z}\Big) = \frac{1}{\lambda^2} \, S(u,v) \Big|_{u=\frac{x}{\lambda z}, v=\frac{y}{\lambda z}}} , \tag{9.39}$$

where $S = \mathcal{F}[s]$ is the 2D FT of the transducer. Recall $k = \omega_0 / c = 2\pi/\lambda$.

Note the importance of accurate notation: we take FT of $s(x,y)$, but *evaluate* the transform at spatial (x,y) arguments.

Ignoring the inner phase term is reasonable if $k r_0^2/(2z) \ll 1$ (radian), *i.e.*,

$$z \gg (\pi/\lambda) r_{0,\max}^2 = D_{\max}^2 / \lambda \cdot (\pi/4) \approx \boxed{D_{\max}^2 / \lambda.}$$

The range $z \geq D_{\max}^2/\lambda$ is called the **far field**.

Example. For a $D = 1$ cm transducer and $\lambda = 1$ mm, need $z \gg 10$ cm.

Under the Fraunhofer approximation, after the usual gain correction, the reflectivity estimate for an A-scan becomes:

$$\hat{R}(0,0,z) = \left| \iiint R(x_1,y_1,z_1) \, \mathrm{e}^{\imath k 2 r_1} \, b_{\text{Fraunhofer}}^2(x_1,y_1,z_1) \, a\left(\frac{2}{c}(z - z_1) \right) \mathrm{d}x_1 \, \mathrm{d}y_1 \, \mathrm{d}z_1 \right| .$$

Example: square transducer

If $s(x,y) = \mathrm{rect}\big(\frac{x}{D}\big) \, \mathrm{rect}\big(\frac{y}{D}\big)$, then $S(u,v) = D^2 \, \mathrm{sinc}(Du) \, \mathrm{sinc}(Dv)$. So the **far-field beam pattern** is

$$b_{\text{Fraunhofer}}(x,y,z) = \frac{1}{\lambda^2} S\Big(\frac{x}{\lambda z}, \frac{y}{\lambda z}\Big) = \left(\frac{D}{\lambda} \right)^2 \mathrm{sinc}\left(\frac{Dx}{\lambda z} \right) \mathrm{sinc}\left(\frac{Dy}{\lambda z} \right) . \tag{9.41}$$

Beam pattern in polar coordinates

So far we treated everything in Cartesian coordinates, mostly as in Macovski.
For beam steering, polar coordinates (for the beam pattern) are probably more natural (for $r - \theta$ **sector scan** format).

We want to simplify the narrowband beam pattern derived in (U.15) above.

$$b^{\text{Cartesian}}_{\text{Narrowband}}(x_1, y_1, z_1) = \frac{\cos\theta_1}{\lambda^2} \iint s(x_0, y_0)\, \mathrm{e}^{\imath k(r_{01} - r_1)}\, \mathrm{d}x_0\, \mathrm{d}y_0 \,.$$

- To simplify analysis, assume source is separable: $s(x, y) = s_{\mathrm{x}}(x)\, s_{\mathrm{y}}(y)$.
- To concentrate on beam pattern in (x, z) plane, consider "thin" (1D) transducer element: $s_{\mathrm{y}}(y) = \delta(y/\lambda) = \lambda\, \delta(y)$. (We need λ for unit balance.)
- Represent (x, z) plane in polar coordinates: $x = r \sin\theta,\ z = r\cos\theta$. (Treat object as 2D, so take $y_1 = 0$.)

Then we define the narrowband **beam pattern** in polar coordinates as:

$$b_{\text{Narrowband}}(r, \theta) \triangleq b^{\text{Cartesian}}_{\text{Narrowband}}(r\sin\theta, 0, r\cos\theta) = \frac{\cos\theta}{\lambda} \int s_{\mathrm{x}}(x)\, \mathrm{e}^{\imath k(d(x;r,\theta) - r)}\, \mathrm{d}x,$$

where $d(x; r, \theta)$ is distance from source point $(x, 0, 0)$ to a point at (r, θ) in $y = 0$ plane:

$$\begin{aligned} d(x; r, \theta) &= r_{01} = \|(x, 0, 0) - (r\sin\theta, 0, r\cos\theta)\| \\ &= \sqrt{(x - r\sin\theta)^2 + (r\cos\theta)^2} = \sqrt{x^2 - 2xr\sin\theta + r^2} = \boxed{r\sqrt{1 - 2\frac{x}{r}\sin\theta + \left(\frac{x}{r}\right)^2}.} \end{aligned}$$

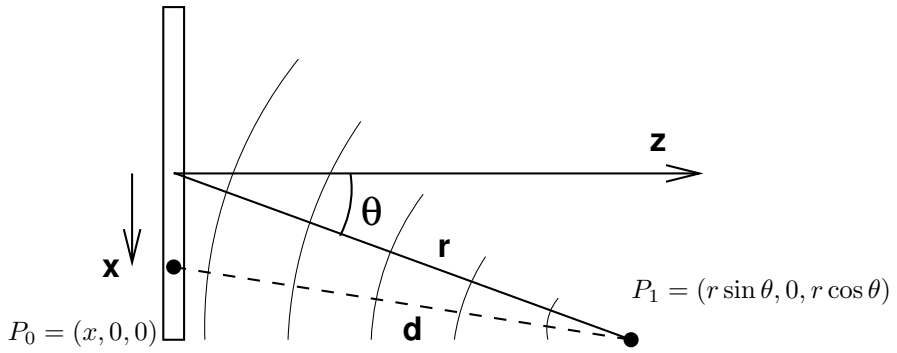

Simplifying approximations: Fresnel and Fraunhofer

The integral above for $b_{\text{Narrowband}}$ is too complicated to provide simple interpretation. To simplify, consider **Taylor series**:

$$f(t) = f(0) + \dot{f}(0)t + \frac{1}{2}\ddot{f}(0)t^2 + \frac{1}{3!}\dddot{f}(0)t^3 + \frac{1}{4!}\ddddot{f}(0)t^4 + \dots,$$

where $t = x/r$, and $\beta = \sin\theta$. One can verify the following.

$f(t) = \sqrt{1 - 2t\beta + t^2}$	$f(0) = 1$	For $\lvert t\rvert < 1$, $1 - \lvert t\rvert \le f(t) \le \lvert t\rvert + 1$
$\dot{f}(t) = (t - \beta)/f(t)$	$\dot{f}(0) = -\beta = -\sin\theta$	$-1 \le \dot{f}(t) \le 1$
$\ddot{f}(t) = (1 - \beta^2)/f^3(t)$	$\ddot{f}(0) = 1 - \beta^2 = \cos^2\theta$	
$\dddot{f}(t) = -3(1 - \beta^2)\dot{f}(t)/f^4(t)$	$\dddot{f}(0) = 3\beta(1 - \beta^2) = 3\sin\theta\cos^2\theta$	
$\ddddot{f}(t) = [-3\ddot{f}^2(t) - 4\dot{f}(t)\dddot{f}(t)]/f(t)$	$\ddddot{f}(0) = 3\cos^2\theta(5\sin^2\theta - 1)$.	

Thus

$$f(t) \approx 1 - t\sin\theta + \frac{1}{2}t^2\cos^2\theta + \frac{1}{2}t^3\sin\theta\cos^2\theta + \frac{3}{4!}t^4\cos^2\theta(5\sin^2\theta - 1).$$

Applying this expansion to d yields

$$\begin{aligned} d(x;r,\theta) &= rf(x/r) \approx r\left[1 - \frac{x}{r}\sin\theta + \frac{1}{2}\left(\frac{x}{r}\right)^2 \cos^2\theta + \frac{1}{2}\left(\frac{x}{r}\right)^3 \sin\theta\cos^2\theta + \frac{3}{4!}\left(\frac{x}{r}\right)^4 \cos^2\theta\left(5\sin^2\theta - 1\right)\right] \\ &\approx \boxed{r - x\sin\theta + \frac{x^2}{2r}\cos^2\theta.} \end{aligned}$$

Physical interpretations:
- r : propagation
- $x\sin\theta$: steering
- $\frac{x^2}{2r}\cos^2\theta$: focusing (curvature of wavefront)

When is this approximation accurate?

Because d enters as $\mathrm{e}^{\imath k\, d}$, we can ignore the 3rd-order (aberration?) term if $kr\frac{1}{2}\left(\frac{x}{r}\right)^3 \sin\theta\cos^2\theta \ll 1$ radian.

The maximum of $\sin\theta\cos^2\theta$ occurs when $\sin^2\theta = 1/3$, so $\left|\frac{1}{2}\sin\theta\cos^2\theta\right| \le 1/3^{3/2}$. Thus $kr\frac{1}{2}\left(\frac{x}{r}\right)^3 \sin\theta\cos^2\theta \le kr\left(\frac{x}{r\sqrt{3}}\right)^3$.

Thus we need $r^2 \gg k(x/\sqrt{3})^3$ or $r \gg \sqrt{k(x/\sqrt{3})^3}$ where x is half the width of (centered) aperture.
E.g., if 10mm wide aperture and $\lambda = 0.5$ mm, then $r \gg 50$ mm.

But 3rd-order term is 0 for $\theta = 0$, so 4th-order term is more important on axis.
For $\theta = 0$, for the 4th-order term to be negligible we need $rk\frac{1}{4!}3(x_{\max}/r)^4 \ll 1$ or $r^3 \gg (2\pi/\lambda)\frac{1}{8}x_{\max}^4 \approx x_{\max}^4/\lambda$ *i.e.*,
$\boxed{r \gg x_{\max}\sqrt[3]{x_{\max}/\lambda}.}$ (*cf.* earlier condition for Fresnel approximation).

Fresnel approximation in polar coordinates (approximate circular wavefront by parabola)

For $r \gg x_{\max}\sqrt[3]{x_{\max}/\lambda}$, we can safely use the above 2nd-order Taylor series approximation: $d(x;r,\theta) - r \approx -x\sin\theta + \frac{x^2}{2r}\cos^2\theta$ leading to the following **Fresnel approximation** to the **beam pattern**:

$$b_{\mathrm{Narrowband}}(r,\theta) \approx b_{\mathrm{Fresnel}}(r,\theta)$$

$$\boxed{b_{\mathrm{Fresnel}}(r,\theta) \triangleq \frac{\cos\theta}{\lambda}\int s_{\mathrm{X}}(x)\,\mathrm{e}^{\imath k(x\cos\theta)^2/(2r)}\,\mathrm{e}^{-\imath kx\sin\theta}\,\mathrm{d}x} \tag{9.38}$$

b_{Fresnel} still messy because it involves a complex exponential with quadratic phase. (Hence no pictures yet...)
It is suitable for computation, but there remains room for refining intuition.

Fraunhofer approximation in polar coordinates

We can ignore 2nd-order term if: $kx_{\max}^2/(2r) \ll 1$, *i.e.*, $r \gg \pi x_{\max}^2/\lambda = \frac{\pi}{4}D^2/\lambda \approx \boxed{D^2/\lambda.}$
If $N = D/\lambda$ (called the **numerical aperture**) then $r \ge ND = D^2/\lambda$ is the **far-field**.
Thus in the far-field we have:

$$b_{\mathrm{Fresnel}}(r,\theta) \approx b_{\mathrm{Fraunhofer}}(\theta)$$

$$\boxed{b_{\mathrm{Fraunhofer}}(\theta) \triangleq \frac{\cos\theta}{\lambda}\int s_{\mathrm{X}}(x)\,\mathrm{e}^{-\imath kx\sin\theta}\,\mathrm{d}x = \frac{\cos\theta}{\lambda}S_X\left(\frac{\sin\theta}{\lambda}\right),} \tag{9.38}$$

where $S_X = \mathcal{F}[s_{\mathrm{X}}]$. In words: *(far-field) angular beam pattern is FT of aperture function*, evaluated at $\sin\theta/\lambda$.

Note the importance of accurate notation: we are take FT of $s(x)$, but *evaluate* the transform at a spatial (x) argument!

The Fraunhofer (far field) beam pattern (in polar coordinates) is *independent of* r.

Example. If $s_{\mathrm{x}}(x) = \mathrm{rect}(x/D)$, then $S_X(u) = D\,\mathrm{sinc}(Du)$ so the **far-field beam pattern** is

$$b_{\mathrm{Fraunhofer}}(\theta) = \frac{\cos\theta}{\lambda} S_X\left(\frac{\sin\theta}{\lambda}\right) = \boxed{\frac{\cos\theta}{\lambda/D}\,\mathrm{sinc}\left(\frac{\sin\theta}{\lambda/D}\right).}$$

Note $x/z = \tan\theta \approx \sin\theta$ and $\cos\theta \approx 1$ for $\theta \approx 0$. So polar and Cartesian approximations are equivalent near axis.

Note $\theta \in (-\pi/2, \pi/2)$, *i.e.*, above approximations are good for any angle, whereas Cartesian good only for small x/z.

The following figure shows $b_{\mathrm{Fraunhofer}}$.

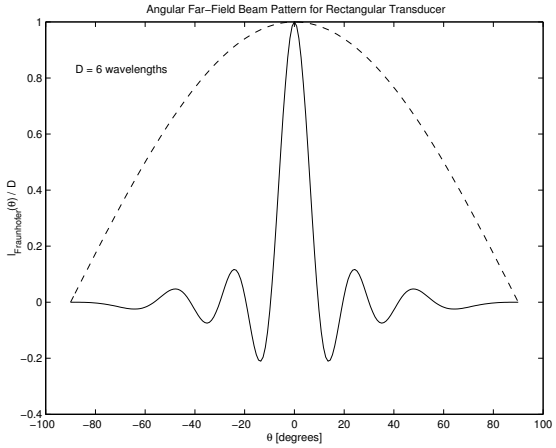

The following figure compares $b_{\mathrm{Fraunhofer}}$ and b_{Fresnel}.

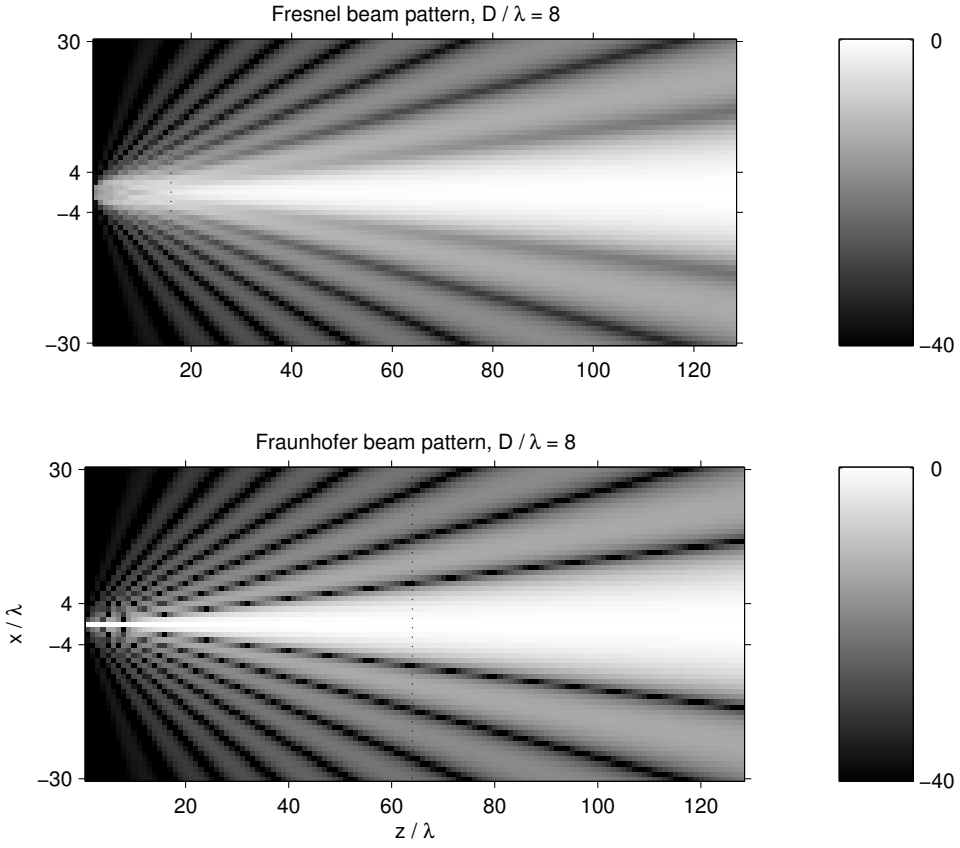

Physical interpretation of beam pattern

We can understand the sinc response physically as well as through the mathematical derivation above.

A point reflector that is on-axis in the far field reflects a pressure wave that is almost a plane wave parallel to the transducer plane by the time it reaches the transducer. Being aligned with the transducer, a large pressure pulse produces a large output voltage.

On the other hand, for a point reflect that is off-axis in the far field, the approximate plane wave hits the transducer at an angle, so there is a (sinusoidal) mix of positive and negative pressures applied to the transducer. If the angle is such that there is an integer number of periods of the wave over the transducer, then there is no net pressure so the output signal is 0. These are the zeros in the sinc function. If the angles is such there is a few full periods and a fraction of a period leftover, there will be a small net positive or negative pressure—this is the sidelobes.

Design tradeoffs

Why did we do all this math? The above simplifications finally led to an easily interpreted form for the lateral response as a function of depth.

The width of the sinc function is about 1, so the (angular) **beam width** is about $\Delta_\theta = \arcsin(\lambda/D)$.
Because $\sin\theta = x/r = x/\sqrt{x^2+z^2} \approx x/z$, the beam width is $\Delta_x = z\Delta_\theta$, or $\boxed{\lambda z/D.}$

How can we use system design parameters to affect spatial resolution?

- Smaller wavelength λ, better lateral resolution (but more attenuation) so SNR decreases.
- Larger transducer gives better far field resolution, (but worse in near field).
- Resolution degrades with depth z (beam spreading)

The Fraunhofer beam pattern is called the **diffraction limited** response, because it represents the best possible resolution for a given transducer. Best possible has two meanings. One meaning is that the *actual* beam pattern will be at least as broad as the Fraunhofer beam pattern, (*i.e.*, a more precise calculation of the beam pattern that includes the phase term $\mathrm{e}^{\imath k r_0^2/(2z)}$ in the integral produces a beam pattern that is no narrower than the Fraunhofer beam pattern). The second is that even if we use a lens to focus, the size of the focal spot (*i.e.*, the width of the beam pattern at the focal plane) will be no narrower than the Fraunhofer beam pattern).

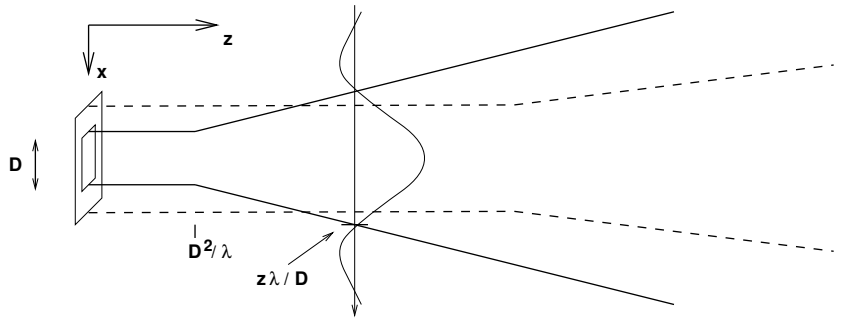

Effective of doubling source size: narrower far-field beam pattern, but wider in near-field.

How to overcome tradeoff between far-field resolution and depth-of-field, *i.e.*, how can we get good near-field resolution even with a large transducer? Answer: by **focusing**.

Approximate beam patterns in Cartesian coordinates

It is also useful to express the Fresnel and Fraunhofer beam patterns (9.38) and (9.38) in Cartesian coordinates. Using the approximation $\sin\theta = x/r \approx x/z$ leads to:

$$b_{\text{Fresnel}}(x,y,z) = \frac{1}{\lambda^2}\iint s(x_0,y_0)\exp\left(\imath\frac{k}{2z}\left[(x-x_0)^2+(y-y_0)^2\right]\right)\mathrm{d}x_0\,\mathrm{d}y_0 \approx \mathrm{e}^{\imath k r^2/(2z)}\, b_{\text{Fraunhofer}}(x,y,z)$$

$$b_{\text{Fraunhofer}}(x,y,z) = \frac{1}{\lambda^2}\iint s(x_0,y_0)\exp\left(-\imath\frac{2\pi}{\lambda z}[xx_0+yy_0]\right)\mathrm{d}x_0\,\mathrm{d}y_0 = \frac{1}{\lambda^2}\,S(u,v)\Big|_{u=\frac{x}{\lambda z},\, v=\frac{y}{\lambda z}} .$$

Time-delay, phase, propagation delay

For a narrowband amplitude modulated pulse, a small time delay τ is essentially equivalent to a phase change:

$$p(t) = a(t)\,\mathrm{e}^{-\imath\omega_0 t} \Longrightarrow p(t-\tau) = a(t-\tau)\,\mathrm{e}^{-\imath\omega_0(t-\tau)} \approx a(t)\,\mathrm{e}^{-\imath\omega_0(t-\tau)} = a(t)\,\mathrm{e}^{-\imath\omega_0 t}\,\mathrm{e}^{\imath\omega_0\tau} = p(t)\underbrace{\mathrm{e}^{\imath\omega_0\tau}}_{\text{phase}}.$$

Another way to modify the phase is to propagate the wave through a material having a different index of refraction, or equivalently a different sound velocity:

$$p(t) \to \left| \begin{array}{c} \leftarrow \delta \rightarrow \\ c_0 \end{array} \right| \to p_0(t) = p(t-\delta/c_0) \approx p(t)\,\mathrm{e}^{\imath\omega_0\delta/c_0} = p(t)\,\mathrm{e}^{\imath 2\pi\delta/\lambda}$$

$$p(t) \to \left| \begin{array}{c} \leftarrow \delta \rightarrow \\ c_1 \end{array} \right| \to p_1(t) = p(t-\delta/c_1) \approx p(t)\,\mathrm{e}^{\imath\omega_0\delta/c_1} = p_0(t)\underbrace{\mathrm{e}^{\imath 2\pi(c_0/c_1-1)\delta/\lambda}}_{\text{phase}}.$$

By varying the thickness δ over the transducer face, one can modify the phase of $s(x,y)$ to make, for example, an acoustic lens.

Focusing ("Mechanically") (1D analysis)

Suppose we choose the thickness δ above as a function of position x along the transducer such that $(c_0/c_1 - 1)\delta = -x^2/2z_f$. Then this is equivalent to modifying the source such that

$$s^{\mathrm{new}}(x) = s^{\mathrm{orig}}(x)\,\mathrm{e}^{-\imath kx^2/(2z_f)}\,.$$

So for $\theta \approx 0$ (so $\cos\theta \approx 1$), the resulting beam pattern is

$$\begin{aligned} b^{\mathrm{new}}_{\mathrm{Fresnel}}(r,\theta) &\approx \frac{\cos\theta}{\lambda}\int s^{\mathrm{new}}(x)\,\mathrm{e}^{\imath kx^2/(2r)}\,\mathrm{e}^{\imath kx\sin\theta}\,\mathrm{d}x \\ &= \frac{\cos\theta}{\lambda}\int s^{\mathrm{orig}}(x)\,\mathrm{e}^{\imath kx^2/2[1/r - 1/z_f]}\,\mathrm{e}^{\imath kx\sin\theta}\,\mathrm{d}x\,. \end{aligned}$$

So in particular for $r \approx z_f$:

$$b^{\mathrm{new}}_{\mathrm{Fresnel}}(r,\theta) \approx \frac{\cos\theta}{\lambda}\int s^{\mathrm{orig}}(x)\,\mathrm{e}^{\imath kx\sin\theta}\,\mathrm{d}x = b^{\mathrm{orig}}_{\mathrm{Fraunhofer}}(\theta)\,.$$

So at depth z_f (and nearby) (even if this z_f is in the near field) the modified system achieves the diffraction limited resolution (of about $\lambda z_f/D$), even for a large transducer.

This **focusing** could be done with a curved acoustic lens of appropriate radius and index of refraction.
In typical lens material, the acoustic waves travel *faster*, *i.e.*, $c_1 > c_0$, so use thickness proportional to x^2 in 1D or $x^2 + y^2$ in 2D.

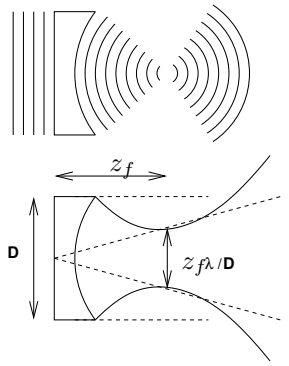

The key point is that this focusing technique works even if z_f is in **near field** of transducer!

What are the drawbacks?

- Worse far-field resolution. (*cf.* distance background in photograph)
- Focal depth z_f is "fixed" by mechanical hardware choice.

F number is z_f/D. If F number large ($\gg 1$), then resolution degrades gradually on either side of focal plane.
But for z_f to small relative to D, the resolution degrades rapidly away from the focal plane.

Phased arrays allow something like this with electronics for variable depth focusing.

Skip wideband diffraction, compound scan

Example. (From Prof. Noll)

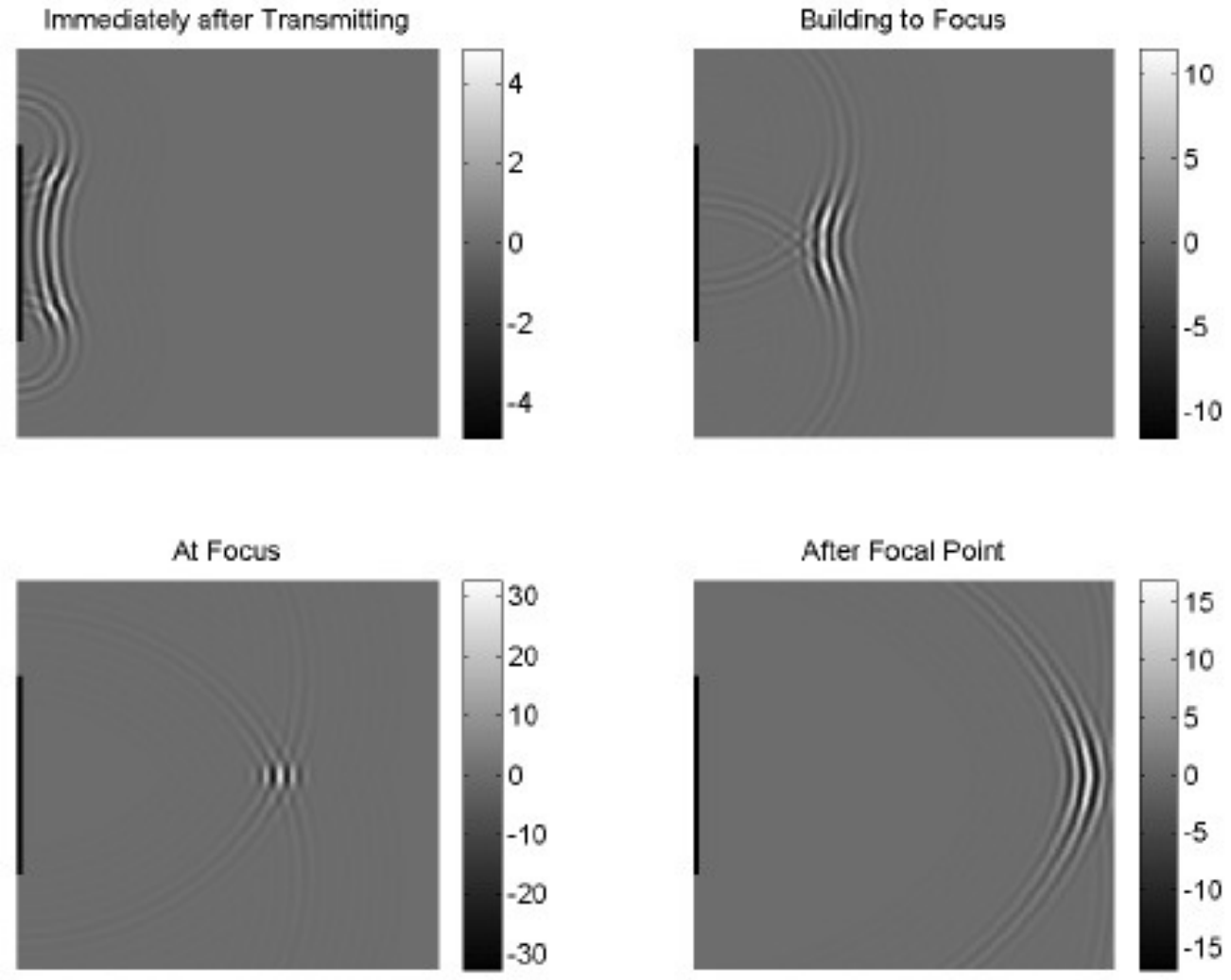

In these images, the transducer is indicated by the black line along the left margin and the transmitted wave is curved to focus at a particular point. Previously, we discussed the depth resolution was determined by the envelope function (in this case a Gaussian). The lateral localization function is more complicated and is determined by diffraction.

Ideal deflection (beam steering)

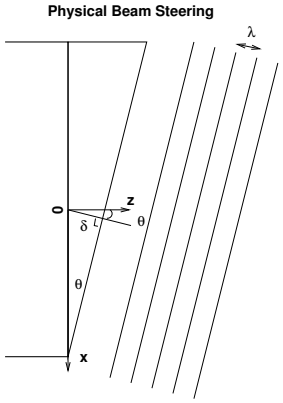

The echo from a far-field reflector will approximate a plane wave impinging on the transducer plane. By using a wedge-shaped piece of material in which the velocity of sound is faster than in tissue, the wave fronts from an angle θ can be made parallel with the transducer so maximum signal from reflectors at that angle.

In particular, suppose we choose δ in the phase/delay analysis above to vary linearly over the transducer face such that

$$(c_0/c_1 - 1)\delta_x = x\beta,$$

where $\beta = \sin\theta_0$ is the desired beam direction.

The equivalent corresponding "time delay" is $\tau_x = (c_0/c_1 - 1)\delta_x/c_0 = x\beta/c_0$.

The resulting "ideal" (1D) beam-steering transducer function would be:

$$s_{\mathrm{x}}^{\mathrm{ideal}}(x) = \mathrm{e}^{\imath 2\pi x\beta/\lambda} \operatorname{rect}\left(\frac{x}{D}\right).$$

Note that there is no change in "amplitude" across transducer, just in phase.

The corresponding **far-field beam pattern** would be:

$$b_{\mathrm{Fraunhofer}}(\theta) = \frac{\cos\theta}{\lambda} S_X^{\mathrm{ideal}}\left(\frac{\sin\theta}{\lambda}\right) = \frac{\cos\theta}{\lambda/D} \operatorname{sinc}\left(D\left(\frac{\sin\theta - \beta}{\lambda}\right)\right) = \frac{\cos\theta}{\lambda/D} \operatorname{sinc}\left(\frac{\sin\theta - \sin\theta_0}{\lambda/D}\right),$$

which is peaked at $\sin\theta = \beta$ *i.e.*, at $\theta = \theta_0$. So steering by phase delays works! Note somewhat larger sidelobes.

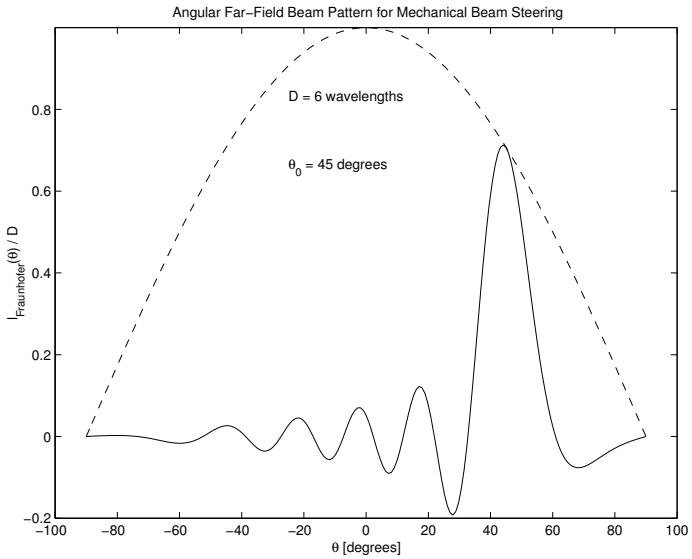

This wedge-shaped acoustic lens (*cf.* prism) is fixed to a single angle θ_0. A phased array allows one to vary the angle electronically in essentially real time.

Speckle "Noise"

Really an artifact because nonrandom in the sense that the same structures appear if scan is repeated under same conditions.
But random in the sense that scatterers are located "randomly" in tissue (*i.e.*, from patient to patient).
Summary: speckle noise leads to Rayleigh statistics and a disappointingly low SNR.

A 1D example

If $R(x,y,z) = \delta(x,y)\, R(z)$ then

$$v_c(t) = \mathrm{e}^{-\imath\omega_0 t} \int R(z')\, \mathrm{e}^{\imath 2kz'}\, a\left(t - \frac{2z'}{c}\right) \mathrm{d}z',$$

and if $R(z) = \sum_l \delta(z - z_l)$ then

$$\hat{R}(z) = \left| v_c\left(\frac{2z}{c}\right)\right| = \left| \int \sum_l \delta(z' - z_l)\, \mathrm{e}^{\imath 2kz'}\, a\left(\frac{2}{c}(z - z')\right) \mathrm{d}z' \right| = \left| \sum_l \mathrm{e}^{\imath 4\pi z_l/\lambda}\, a\left(\frac{2}{f_0}\frac{(z - z_l)}{\lambda}\right)\right|.$$

For subsequent analysis, it is more convenient to express in terms of wavelengths. Let $w = z/\lambda$, $w_l = z_l/\lambda$, $h(w) = a(2w/f_0)$,

$$\hat{R}(w\lambda) = \left| \sum_l \mathrm{e}^{\imath 4\pi w_l}\, h(w - w_l)\right|.$$

Without phase term we would just get superposition of shifted h functions. But with it, we get destructive interference.

Example.

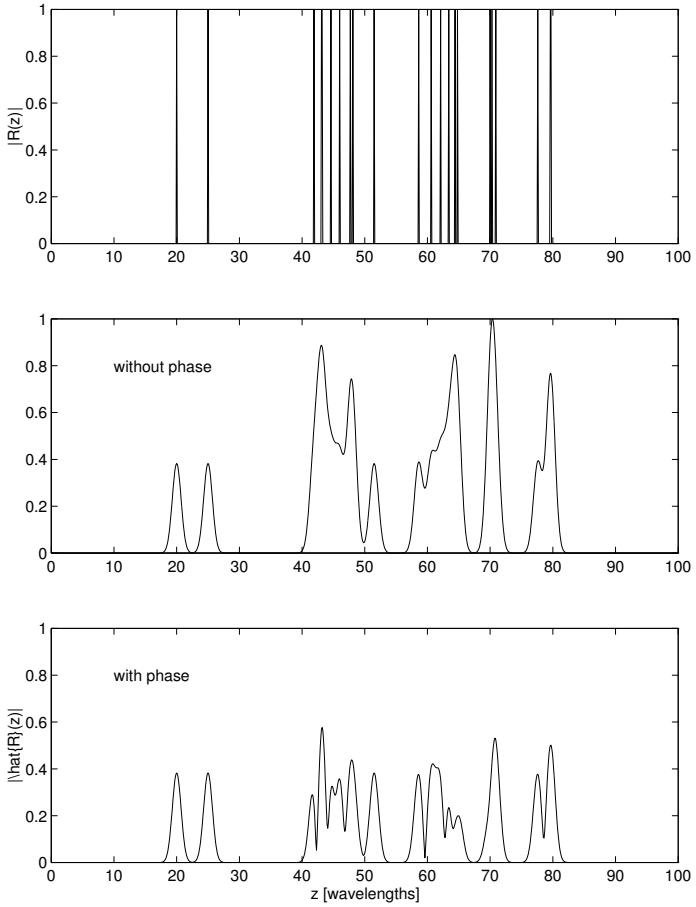

How can we model this phenomena so as to characterize its effects on image quality? Statistically!

Rayleigh distribution

From [9, Ex. 4.37, p. 229], if U and V are two zero-mean, unit-variance, independent Gaussian random variables, then $W = \sqrt{U^2 + V^2}$ has a Rayleigh distribution:

$$f_W(w) = w \, \mathrm{e}^{-w^2/2} \; 1_{\{w \geq 0\}}$$

for which $\mathsf{E}[W] = \sqrt{\pi/2}$ and $\sigma_W^2 = 2 - \pi/2$.

Rayleigh statistics of sum of random phasors (For ultrasound speckle)

To examine the properties of $\hat{R}(z)$ for some given z, we assume the pulse envelope is broad enough that it encompasses several, say n, scatterers, at positions $w_1, \ldots, w_n$. We can treat those positions as independent random variables, and a reasonable model is that they have a uniform distribution. Thus it is reasonable to model the corresponding phases $\Theta_l = 4\pi w_l$ as i.i.d. random variables with Uniform$(0, 2\pi)$ distributions. For a sufficiently broad envelope, we can treat $h(\cdot)$ as a constant and consider the following model for the envelope of a signal that is sum of many random phasors:

$$W_n = \sqrt{\frac{2}{n}} \left| \sum_{l=1}^{n} \mathrm{e}^{\imath \Theta_l} \right| .$$

Mathematically, this is like a **random walk** on the complex plane.

Goal: to understand statistical properties of W_n (and hence $\hat{R}$). We will show that W_n is approximately Rayleigh distributed for large n. Expanding:

$$W_n = \sqrt{\frac{2}{n}} \left| \sum_{l=1}^{n} \mathrm{e}^{\imath \Theta_l} \right| = \sqrt{\frac{2}{n}} \left| \sum_{l=1}^{n} \cos \Theta_l + \imath \sum_{l=1}^{n} \sin \Theta_l \right| = \sqrt{U_n^2 + V_n^2}$$

where

$$U_n \triangleq \sqrt{\frac{2}{n}} \sum_{l=1}^{n} \cos \Theta_l, \qquad V_n \triangleq \sqrt{\frac{2}{n}} \sum_{l=1}^{n} \sin \Theta_l .$$

Note $\mathsf{E}[U_n] = \mathsf{E}[V_n] = 0$ because $\mathsf{E}[\cos(\Theta + c)] = 0$ for any constant c, when Θ has a uniform distribution over $[0, 2\pi]$. (See [9, Ex. 3.33, p. 131].) Also, $\mathsf{Var}\{U_n\} = 2\,\mathsf{Var}\{\cos \Theta\}$ because i.i.d., where

$$\mathsf{Var}\{\cos \Theta\} = \mathsf{E}\left[(\cos \Theta - \mathsf{E}[\Theta])^2 \right] = \int_{-\infty}^{\infty} (\cos \theta - \mathsf{E}[\Theta])^2 f_\Theta(\theta) \, \mathrm{d}\theta = \int_0^{2\pi} \frac{1}{2\pi} \cos^2 \theta \, \mathrm{d}\theta = \int_0^{2\pi} \frac{1}{2\pi} \frac{1}{2} \left(1 + \cos(2\theta)\right) \mathrm{d}\theta = \frac{1}{2}.$$

Thus $\mathsf{Var}\{U_n\} = \mathsf{Var}\{V_n\} = 1$. Furthermore, U_n and V_n are uncorrelated: $\mathsf{E}[U_n V_n] = 2\,\mathsf{E}[\cos \Theta \sin \Theta] = 0$.

So to show that $\sqrt{U_n^2 + V_n^2}$ is approximately Rayleigh distributed, all that is left for us to show is that for large n, U_n and V_n are approximately (jointly) normally distributed.

Bivariate central limit theorem (CLT) [10, Thm. 1.4.3]

Let (X_k, Y_k) be i.i.d. random variables with respective means μ_X and μ_Y, variances σ_X^2 and σ_Y^2, and correlation coefficient ρ, and define

$$\vec{Z}_n = \begin{bmatrix} \frac{1}{\sqrt{n}} \sum_{k=1}^{n} \frac{X_k - \mu_X}{\sigma_X} \\ \frac{1}{\sqrt{n}} \sum_{k=1}^{n} \frac{Y_k - \mu_Y}{\sigma_Y} \end{bmatrix} .$$

As $n \to \infty$, $\vec{Z}_n$ converges in distribution to a bivariate normal random vector with zero mean and covariance

$$\begin{bmatrix} 1 & \rho \\ \rho & 1 \end{bmatrix} .$$

In particular, if $\rho = 0$, then as $n \to \infty$, the two components of $\vec{Z}_n$ approach independent Gaussian random variables.

Hence statistics of speckle often assumed to be Rayleigh.

Signal to noise ratio (signal mean over signal standard deviation)

$$\mathsf{SNR} = \frac{\mathsf{E}[W]}{\sigma_W} = \frac{\sqrt{\pi/2}}{\sqrt{2 - \pi/2}} = \sqrt{\frac{\pi}{4 - \pi}} \approx 1.91 \tag{9.72}$$

Low ratio! Averaging multiple (identically positioned) scans will not help. One can reduce speckle noise by **compounding**, meaning combining scans *taken from different directions* so that the distances r_{01}, and hence the phases, are different, *e.g.*, [11].

See [12] for further statistical analysis of envelope detected RF signals with applications to medical ultrasound.

Summary

- Introduction to physics of ultrasound imaging
- Derivation of of "signal equation" relating quantity of interest, reflectivity $R(x, y, z)$, to the recorded signal $v(t)$.
- Description of (simple!) image formation method for A-mode scan and B-mode scans.
- Analysis of (depth dependent!) point spread function
- Analysis of (speckle) noise

Bibliography

[1] T. L. Szabo. *Diagnostic ultrasound imaging: Inside out*. academic, New York, 2004.

[2] K. K. Shung, M. B. Smith, and B. Tsui. *Principles of medical imaging*. Academic Press, New York, 1992.

[3] J. L. Prince and J. M. Links. *Medical imaging signals and systems*. Prentice-Hall, 2005.

[4] D. I. Hughes and F. A. Duck. Automatic attenuation compensation for ultrasonic imaging. *Ultrasound in Med. and Biol.*, 23:651–64, 1997.

[5] J. W. Goodman. *Introduction to Fourier optics*. McGraw-Hill, New York, 1968.

[6] M. Born and E. Wolf. *Principles of optics*. Pergamon, Oxford, 1975.

[7] A. D. Pierce. *Acoustics; An introduction to its physical principles and applications*. McGraw-Hill, New York, 1981.

[8] A. Macovski. *Medical imaging systems*. Prentice-Hall, New Jersey, 1983.

[9] A. Leon-Garcia. *Probability and random processes for electrical engineering*. Addison-Wesley, New York, 2 edition, 1994.

[10] P. J. Bickel and K. A. Doksum. *Mathematical statistics*. Holden-Day, Oakland, CA, 1977.

[11] G. M. Treece, A. H. Gee, and R. W. Prager. Ultrasound compounding with automatic attenuation compensation using paired angle scans. *Ultrasound in Med. Biol.*, 33(4):630–42, 2007.

[12] R. F. Wagner, M. F. Insana, and D. G. Brown. Statistical properties of radio-frequency and envelope detected signal with applications to medical ultrasound. *J. Opt. Soc. Am. A*, 4(5):910–22, 1987.